Cancer Investigation, 30:343–363, 2012
ISSN: 0735-7907 print / 1532-4192 online
DOI: 10.3109/07357907.2012.664670

informa
healthcare

CELLULAR AND MOLECULAR BIOLOGY

High-Throughput Molecular and Histopathologic Profiling of Tumor Tissue in a Novel Transplantable Model of Murine Neuroblastoma: New Tools for Pediatric Drug Discovery

Jimmy K. Stauffer,[1] Rimas J. Orentas,[1] Erin Lincoln,[2] Tahira Khan,[1] Rosalba Salcedo,[1] Julie A. Hixon,[1] Timothy C. Back,[2] Jun S Wei,[3] Rajesh Patidar,[3] Young Song,[3] Laura Hurd,[3] Maria Tsokos,[4] Edwin W. Lai,[5] Graeme Eisenhofer,[5] William Weiss,[6] Javed Khan,[1,3] and Jon M. Wigginton[1]

Pediatric Oncology Branch, Center for Cancer Research, National Cancer Institute, Bethesda, MD, USA,[1] Basic Research Program, SAIC-Frederick, Inc., NCI at Frederick, Frederick, Maryland, USA,[2] Oncogenomics Section, Pediatric Oncology Branch, Advanced Technology Center,[3] Laboratory of Pathology, Center for Cancer Research, National Cancer Institute, Bethesda, Maryland, USA,[4] National Institute of Neurologic Disorders and Stroke, Bethesda, Maryland, USA,[5] Department of Neurology, University of California-San Francisco, San Francisco, California, USA[6]

Cancer Invest Downloaded from informahealthcare.com by NIH Pathology Lab on 11/12/14
For personal use only.

Using two MYCN transgenic mouse strains, we established 10 transplantable neuroblastoma cell lines via serial orthotopic passage in the adrenal gland. Tissue arrays demonstrate that by histochemistry, vascularity, immunohistochemical staining for neuroblastoma markers, catecholamine analysis, and concurrent cDNA microarray analysis, there is a close correspondence between the transplantable lines and the spontaneous tumors. Several genes closely associated with the pathobiology and immune evasion of neuroblastoma, novel targets that warrant evaluation, and decreased expression of tumor suppressor genes are demonstrated. These studies describe a unique and generalizable approach to expand the utility of transgenic models of spontaneous tumor, providing new tools for preclinical investigation.

Keywords: Neuroblastoma; Mouse model; MYCN; Microenvironment

INTRODUCTION

Despite dramatic success in the treatment of children with many hematologic malignancies, the prognosis of patients with solid tumors including metastatic osteogenic sarcoma, Ewing's sarcoma, and neuroblastoma remains poor overall (1). Among these tumors, neuroblastoma is the most common extracranial solid tumor in children (1). Despite recent progress in the treatment of high-risk neuroblastoma patients using regimens that include surgery, radiotherapy, multiagent chemotherapy with hematopoietic reconstitution, and various biologics to eradicate minimal residual disease, the prognosis of these children is poor overall (2–4). There remains an urgent need then for the development of new therapeutic approaches for these high-risk patients. To more effectively investigate the biology of neuroblastoma tumors and define new strategies for treatment, a significant need exists for expanded flexibility in the scope of existing preclinical model systems (5).

Current preclinical neuroblastoma models emphasize transplantable human tumor cell lines implanted as xenografts into immunodeficient mice, often in a heterotopic subcutaneous site (5). Xenograft models offer obvious advantages for investigating small molecule agents that act directly on targets within the tumor cell itself, and where dosing is guided predominantly by pharmacokinetic/pharmacodynamic considerations. Nonetheless, xenograft models may be less informative or inappropriate in some situations. These include the investigation of therapeutic agents that depend on the presence of an intact immune system or protein-based therapeutics that modulate targets in the host, where efficacy may be compromised by species-specific barriers to interaction between the agent and its target(s). In these circumstances, syngeneic models of murine neuroblastoma using cell lines such as NSX2 (generated from a fusion to C57/BL6 ganglia and thereby actually an allogeneic model) (6, 7), Neuro-2a (8, 9), and TBJ (10, 11) have been used most extensively. Despite their broad use in syngeneic transplantable tumor models, these lines have not been well characterized with respect to their histopathologic and molecular features. Further, despite the relationship between the presence of *MYCN* amplification with neuroblastoma tumors and adverse biologic features and outcome for patients with neuroblastoma (12, 13), the

The authors Jimmy K. Stauffer and Rimas J. Orentas contributed equally to this work.
This article is not subject to United States copyright laws.

Correspondence to: Javed Khan, Oncogenomics Section, Pediatric Oncology Branch, Advanced Technology Center, Center for Cancer Research, National Cancer Institute, 8717 Grovemont Circle, Room 134E, Gaithersburg, MD 20877, USA. email: khanjav@mail.nih.gov

Copyright Informa Healthcare 2011
Not for Sale or Commercial Distribution
Unauthorised use prohibited.
Authorised users can download,
display, view and print a single
copy for personal use
RIGHTSLINK

relationship of MYCN to the origin and pathobiology of existing murine neuroblastoma cell lines remains unclear.

To establish a model of spontaneous murine neuroblastoma with more clearly defined molecular features, a MYCN transgenic mouse has been developed and characterized (14). In these mice, tissue-specific overexpression of the MYCN oncogene under the control of a tyrosine hydroxylase promoter induces spontaneous neuroblastoma tumors in the adrenal glands and the paraspinal sympathetic chain ganglia (14). Amplification of the *MYCN* proto-oncogene has been estimated to occur in up to 30%–40% of children with advanced neuroblastoma tumors (1), and the presence of MYCN amplification within these tumors is associated with rapid disease progression and adverse prognosis (12, 13). MYCN transgenic mice afford the opportunity to investigate the biology and therapeutic responsiveness of spontaneous neuroblastoma tumors that evolve in a host conditioned by the complete dynamic process of neoplastic progression and tumorigenesis. Nonetheless, incomplete tumor penetrance, heterogeneity in the timing of tumor emergence, and technical obstacles to early detection of tumors that develop in occult sites can limit the practical utility of the MYCN transgenic mouse model for preclinical drug development.

To address these potential limitations, we have now established a novel panel of transplantable neuroblastoma cell lines derived from spontaneous tumors that arise in MYCN transgenic mice, and have conditioned these lines for orthotopic transplantation via serial passage in the murine adrenal gland. The present report describes our subsequent histopathologic and molecular profiling of orthotopic tumors established using these lines, comparison of the lines to spontaneous tumors that arise in MYCN transgenic mice, and characterization of the *in vivo* behavior of these tumors. Collectively, these studies demonstrate that tumors established by implantation of these cell lines closely reflect the molecular features and biology of human neuroblastoma tumors, and provide important new investigative tools for pediatric oncology drug discovery, including novel approaches for the treatment of neuroblastoma.

Cancer Invest Downloaded from informahealthcare.com by NIH Pathology Lab on 11/12/14
For personal use only.

MATERIALS AND METHODS

Mouse strains

Breeder pairs of MYCN transgenic mice with the C57BL6/J (TH-MYCN-C57BL6/J) and 129svIM/J (TH-MYCN-129svIM/J) backgrounds were generously provided by Dr. William Weiss (University of California-San Francisco, San Francisco, CA), and colonies of these respective strains were established by the breeding of MYCN+ sibling littermates. These MYCN transgenic mice constitutively overexpress the human MYCN oncogene under the control of a tyrosine hydroxylase promoter (14). As a consequence of tissue-specific overexpression of MYCN, these mice develop spontaneous neuroblastoma tumors in the adrenal gland and/or the paraspinal sympathetic chain ganglia. For breeding purposes, MYCN expression in the respective mice was confirmed by Southern blot analysis as described in the following section, and the colony was maintained by breeding MYCN-positive mice. Where indicated, wild-type control C57BL6/J and 129sv/J mice and C57BL/6-TgN(ACTbEGFP)1Osb transgenic mice purchased from The Jackson Laboratory (Bar Harbor, ME) were utilized. The C57BL6-TgN(ACTbEGFP)1Osb transgenic strain ubiquitously overexpresses the green fluorescent protein (GFP) under the control of a chicken beta-actin promoter and a cytomegalovirus enhancer. GFP is easily detectable in virtually all tissues (including vasculature) except the hair and erythrocytes (15). For all strains, mice were maintained under pathogen-free conditions, and animal care was provided in accordance with the procedures outlined in the *Guide for the Care and Use of Laboratory Animals* (NIH Publication No. -23, 1985).

Southern blot analysis of MYCN expressionTail DNA was extracted using the DNeasy kit (Qiagen, Valencia, CA) according to the manufacturer's protocol and then quantitated by spectrophotometry. Ten micrograms of purified genomic DNA was digested overnight with EcoRI and DNA was resolved by agarose gel electrophoresis. The DNA was then alkaline transferred to nylon membranes (Nytran SuPerCharge, Schleicher and Schuell, Keene, NH) using a rapid downward transfer system (Turboblotter, Schleicher and Schuell, Keene, NH), using manufacturer's protocol. A human MYCN cDNA (gift of W. Weiss) insert was gel purified and labeled using the random primer method (rediprime II, Amersham Pharmacia Biotech, Piscataway, NJ). Membranes and probe were hybridized at 42°C overnight in 50% formamide, 10% dextran sulfate, and 1% SDS (Hybrisol I, Serologicals Corporation, Norcross, GA) followed by high stringency wash at 65°C with 0.2XSSC/0.2% SDS and autoradiographed according to standard protocols. Under these conditions, a single strong EcoRI-hybridized fragment is detected at 1.8 kilobases, representing the human MYCN transgene with no cross hybridization to nontransgenic DNA samples.

Derivation of POB CM and POB UN series orthotopic transplantable neuroblastoma cell lines

To establish the respective POB UN and POB CM series transplantable neuroblastoma cell lines derived from spontaneous tumors in MYCN transgenic mice, cohorts of mice with the C57BL6/J (TH-MYCN-C57BL6/J) and 129svIM/J (TH-MYCN-129svIM/J) backgrounds were monitored for the emergence of spontaneous tumors. When a spontaneous tumor was detectable by palpation and/or abdominal distension, mice were euthanized and individual spontaneous tumors were resected, physically disaggregated, and filtered through sterile mesh to produce single cell suspensions in phosphate-buffered saline (PBS). Cohorts of 5–10 syngeneic wild-type C57BL6/J or 129svIM/J mice were subsequently injected intra-adrenally as described next with 2.0×10^5 to 5.0×10^5 tumor cells in 30 μL PBS (POB UN series and POB CM series, respectively). The resulting cohort of tumor-bearing mice was then euthanized via CO_2 asphyxiation, tumor was resected, and pooled single cell suspensions were prepared as described earlier in the article. This process was repeated 4–5 times until 100% tumor take for a given line was estab-

RIGHTSLINK

lished with successive passages, and large stocks of cells were then cryopreserved utilizing standard techniques. Thus, all tumors were of a similar *in vivo* passage number. To perform the comparative molecular and histopathologic studies described next, tumor cells were then implanted as described earlier and then subjected to 4–5 serial passages in cohorts of 12 wild-type C57BL6/J and 129svIM/J mice for POB UN and POB CM series cell lines, respectively. Mice bearing well-established tumors were then euthanized and tumors were resected and preserved for subsequent histologic or molecular studies by either snap freezing on dry ice, embedding in OCT, fixation in 70% ethanol or formalin, or fixation in a solution consisting of 4% paraformaldehyde, 2% glutaraldehyde, and 0.1 M sodium cacodylate for electron microscopy as specified later in the article. Matched normal tissues including spleen, liver, brain, lung, heart, and skin were also harvested from syngeneic mice and were preserved under similar conditions.

In vivo tumor models

Orthotopic intra-adrenal POB CM and POB UN series tumors were established by surgical exposure and direct injection of tumor cell suspension into the adrenal gland (2×10^5 cells in 30 μL PBS) of syngeneic 129svIM/J and C57BL6/J mice, respectively, using methods we have described previously in detail (16, 17). Disseminated tumor metastases were established, where indicated, by injection of 2×10^5 tumor cells in 200 μL PBS intravenously (IV) into the tail vein of syngeneic mice as previously described (16, 17). Selective hepatic metastases were established, where indicated, by surgical exposure and slow direct intrasplenic injection of 2.5×10^5 tumor cells in 500 μL PBS using methods we have previously described (17). For all molecular and histolopathologic analyses of orthotopic intra-adrenal transplantable tumor implants, established tumors were allowed to progress to an advanced stage before harvest as described earlier. Where indicated, lungs and livers were harvested from mice bearing either disseminated (IV) or selective hepatic (IS)-induced tumor metastases, and organs were then weighed and/or placed into Bouin's fixative for assessment of tumor burden. For fluorescent imaging of tumor vascularity, we utilized a subline of POB UN0092 that had been conditioned for subcutaneous (SC) implantation by a short-term serial SC passage in sublethally irradiated (transient immunocompromised) mice followed by serial passage in wild-type C57BL6/J mice. These POB UN0092 cells were injected SC in the right mid-flank of C57BL/6-TgN(ACTbEGFP)1Osb transgenic mice at a concentration of 5×10^6 cells in 200 μL PBS. Tumor implants were allowed to grow for 17 days to become well established, and mice were then euthanized and subjected to immediate *in situ* fixation with retro-orbital perfusion of 4% paraformaldehyde, as previously described, to optimize preservation of the GFP signal (18). The fixed tumors were then sectioned and counterstained with DAPI to visualize nuclear morphology within the respective tumor and endothelial cell populations, and images of tumor sections were captured by fluorescence microscopy as described in the following sections. Using this approach, tumor implants were vascularized by host-derived vessels that constitutively express GFP (green fluorescent), and counterstaining with DAPI allows for simultaneous imaging of nuclear morphology (blue) within tumor sections.

Tissue array and immunohistochemistry

Tissue arrays containing sections of established POB CM and POB UN series transplantable tumors and paired normal control tissues from these mice were constructed by the Pathology/Histotechnology Laboratory (PHL) at NCI-Frederick (Frederick, MD) to ensure uniformity of conditions for tumors and controls. Initially, hematoxilin and eosin-stained formalin-fixed paraffin-embedded sections of selected tumors and paired normal control tissues (including brain, heart, spleen, liver, lung, and skin) were examined and representative areas were identified for core sampling. Four to eight 0.6 mm cores per donor tissue were assembled into the recipient block and 5-μm serial sections were obtained for subsequent processing and staining as outlined in later sections. TMA slides were deparaffinized with xylene, rehydrated with alcohol, and then subjected to antigen retrieval by two microwave cycles (boiling) in 10 mM citrate (pH 6.0). Formalin-fixed TMA slides were subjected to immunohistochemical (IHC) staining using ABC reagent kit (Vector Laboratories, Burlingame, CA) for markers commonly observed to be expressed in human neuroblastoma tumors. Slides were stained with antibodies including rabbit antihuman synaptophysin (DakoCytomation, Carpinteria, CA; 1:100 dilution), rabbit antibovine chromogranin A (Immunostar, Inc., Hudson, WI; 1:1,000 dilution), rabbit antimouse tyrosine hydroxylase (Chemicon, Temecula, CA; 1:100 dilution), rabbit antimouse cyclin-dependent kinase 4 (Santa Cruz Biotechnology, Santa Cruz, CA; 1:7,500 dilution), rabbit antirat neurofilament H (Chemicon, Temecula, CA; 1:500 dilution), and rabbit antibovine neuron-specific enolase (DAKO, Carpinteria, CA; 1:2,000 dilution). Immunohistochemical staining for the vascular endothelial marker CD31 was also performed using tumor sections preserved in OCT as described earlier and rat antimouse CD31 antibody (Pharmingen, San Diego, CA; 5 μg/mL).

Catecholamine analysis

Tumor specimens for each of the respective POB CM and POB UN series cell lines and selected spontaneous MYCN transgenic tumors, as well as tumors established using TBJ and Neuro-2a murine neuroblastoma and Renca murine renal cell carcinoma (as a negative control) cell lines, were assayed for catecholamine content/production. Established tumor specimens were resected and snap frozen for later use. Samples of snap-frozen tumor tissues were weighed and homogenized in a minimum of 4 volumes of ice-cold 0.4 M perchloric acid containing 0.5 mM EDTA. Tissue homogenates were centrifuged at 4°C, and supernatants were then stored at −70°C for subsequent assay of catecholamine content. Catecholamines including norepinephrine, epinephrine, dopamine, 3,4-dihydroxyphenylalanine (DOPA), 3,4-dihydroxyphenylacetic acid (DOPAC), and 3,4-dihydroxyphenylglycol (DHBG) were extracted from tissue supernatants using an alumina extraction procedure and

Cancer Invest Downloaded from informahealthcare.com by NIH Pathology Lab on 11/12/14
For personal use only.

RIGHTSLINK

quantified by liquid chromatography with electrochemical detection as previously described (19).

Fluorescent imaging

Imaging of GFP-positive vasculature and DAPI-stained tumor cell nuclei in POB CM and POB UN tumor sections was carried out as previously described (20). Briefly, animals were euthanized and tissues immediately fixed *in situ* by retro-orbital perfusion with 4% paraformaldehyde. Tumors were then resected and stored in 4% paraformaldehyde overnight followed by equilibration in 18% sucrose/PBS at 4°C (24 hr). Tissues were then embedded in OCT and cryostated into 10–20 μm sections onto coverslips and counterstained with DAPI upon final mounting. A Nikon Eclipse E400 equipped with epifluorescence illumination was used for high-power (100× magnification) fluorescence microscopy with the fluorescence excitation and emission filter combinations for GFP, excitation source 480 nm/emission filter 505 nm, and DAPI, excitation source 355 nm/emission filter 400 nm.

Electron microscopy

To investigate the ultrastructural histology of POB CM and POB UN series tumors, established tumors were generated as described earlier and then resected and preserved in fixative consisting of 4% paraformaldehyde, 2% glutaraldehyde, and 0.1 M sodium cacodylate. Tumor specimens were then trimmed into 3–4 mm^3 pieces with a single-edged razor blade, post fixed in 1% osmium (Stevens Metallurgical Corp., New York, NY), and embedded in epoxy resin LX-110 (Ladd Research Industries, Inc., Burlington, VT). The embedded tissue was then sectioned to approximately 50–60 nm and mounted on a one-hole grid. The thin sections were stained in uranyl acetate and lead citrate solution to enhance the contrast, stabilized by carbon evaporation in a vacuum evaporator (Denton Vacuum, Inc., Moorestown, NJ), and examined and photographed with an H7000 electron microscope (Hitachi Ltd., Tokyo, Japan) as previously described (21).

Microarray analysis

To further define the molecular features of these neuroblastoma tumors, we utilized cDNA microarray to profile the patterns of gene expression within both spontaneous MYCN transgenic tumors and transplantable orthotopic intra-adrenal POB CM and POB UN series tumors. Established tumors and normal tissue specimens were resected from euthanized mice as described earlier, and then snap frozen in liquid nitrogen. Total RNA was purified using a combination of Trizol extraction followed by Qiagen column purification as previously described (22). RNA integrity was validated in all samples using an Agilent Biolyzer 2100 (Agilent Technologies, Inc., Palo Alto, CA). RNA was amplified by a modified Eberwine RNA amplification procedure (23). Indirect fluorescent labeling of the cDNA probes was done using the amino allyl method (24). Hybridization, washing, and array scanning were performed as previously described (25, 26). For these studies, we utilized a murine cDNA microarray chip consisting of 19,940 detector elements representing 13,958 nonredundant genes. A single internal reference NIH3T3 RNA standard was used in all hybridizations. For comparison purposes, we generated RNA from a diverse panel of tissues to represent a normal expression range by averaging the data from each tissue type from 2 to 7 sets each of syngenic normal tissues including brain, heart, lung, rib cage, spleen, liver, and kidney. To select the genes that were highly overexpressed or underexpressed in serial lines of neuroblastoma compared with the normal tissue samples, the ratios of each serial line of neuroblastoma and normal tissues over a common reference (NIH3T3 cell line) were subjected to SAM analysis (27). Briefly, genes with twofold difference between the mean ratios of the respective POB CM and POB UN series tumors and those of the normal tissues were selected with a false discovery rate of 0.0068%. The mean ratios of each kind of tissues were taken as the representative ratio from the corresponding tissue samples to avoid the bias of tissue types due to difference in the number of sample datasets of the same kind included in the analysis. Unsupervised hierarchical clustering (HC) and principal component analysis (PCA) computations were carried out in MATLAB (MathWorks Inc., Natick, MA).

Quantitative RT-PCR

To validate the microarray results of these neuroblastoma tumors, we performed real-time RT-PCR using Taqman assays on a Fluidigm system according to the manufacturer's real-time RT-PCR protocol (Fluidigm, San Francisco, CA) for 24 tumors including spontaneous MYCN transgenic tumors (CM series) as well as transplantable orthotopic intra-adrenal from the POB CM and POB UN series tumors and 23 normal samples as described earlier. Briefly, 200 ng of RNA was converted to cDNA using SuperScript II reverse transcriptase (Invitrogen, Carlsbad, CA) by random priming. Real-time RT-PCR was carried out on a 48.48 Dynamic Array using BioMark HD real-time PCR system (Fluidigm, San Francisco, CA). Triplicates were performed for each gene for every sample, and average Ct numbers were calculated. Gene expression levels were represented by normalized Ct (δCt) against GAPDH. Fold changes were calculated as $2^{-\Delta\Delta Ct}$ using median ΔCt for tumor ($n = 24$) or normal tissue ($n = 23$) groups. Welch's t-test was used for the calculation of p values. Taqman gene expression assays were purchased from Applied Biosystems (LifeTech, Foster City, CA). Taqman assay IDs are as follows: Cdk4 (Mm00726334_s1), Slit2 (Mm00662153_m1), Birc5 (Mm00599749_m1), Aurka (Mm01248177_m1), Mcm2 (Mm00484804_m1), Plk1 (Mm00440924_g1), Chek1 (Mm01176757_m1), Foxo1 (Mm00490672_m1), Clu (Mm00442773_m1), Ccnd1 (Mm00432359_m1), and GAPDH (Mm99999915_g1).

In vivo growth characteristics

To compare the *in vivo* growth characteristics of the respective POB CM and POB UN series tumors, mice were injected IA with 2×10^5 tumor cells as described earlier (10 mice per group), and were then monitored for survival. As indicated, three mice bearing POB CM 0002 tumors and one mouse bearing a POB UN 0451 tumor were censored from

Cancer Invest Downloaded from informahealthcare.com by NIH Pathology Lab on 11/12/14
For personal use only.

RIGHTSLINK

the analysis for nontumor-related reasons. The ability of the respective POB CM and POB UN series cell lines to form induced hepatic metastases was assessed in mice (10 per group) injected with tumor cells either IV or IS as described earlier (IS: 2.5×10^5 tumor cells/animal, IV: 2.5×10^5 tumor cells/animal). Mice were euthanized when premoribund as described earlier, and livers were resected and placed into Bouin's fixative for later inspection and determination of metastatic disease burden.

RESULTS

Origin of transplantable cell lines

To establish the transplantable neuroblastoma cell lines, we resected spontaneous primary intra-adrenal neuroblastoma tumors from MYCN transgenic mice. For some tumors, single cell tumor cell suspensions were subsequently prepared as described in "Materials and Methods" section, and the respective cell lines were conditioned for transplantation via serial orthotopic intra-adrenal passage. Using this approach, we have derived a total of 10 transplantable tumor cell lines from tumors arising in MYCN transgenic mice with the 129svIMJ background (POB CM series cell lines), and 5 of these respective lines are included in the present report. Seven transplantable tumor cell lines were derived from tumors arising in MYCN transgenic mice with the C57BL/6J background (POB UN series cell lines), and 5 of these lines are included in this report.

Establishment of tissue arrays and basic morphology of neuroblastoma tumors

We initially investigated the basic morphologic features of established orthotopic intra-adrenal POB CM and POB UN series murine neuroblastoma tumors. Tissue arrays were established using formalin-fixed tumor specimens, and sections were stained with hematoxylin and eosin and imaged at 200× (Figure 1(A)) and 100× (Figure 1(B)). Hematoxylin- and eosin-stained sections of these cell lines demonstrate small round blue cell tumors with dense hyperchromatic nuclei and relatively scant cytoplasm (Figures 1(A) and (B)). Some tumor specimens (UN451) contained a mixture of both mature differentiated elements along with large areas

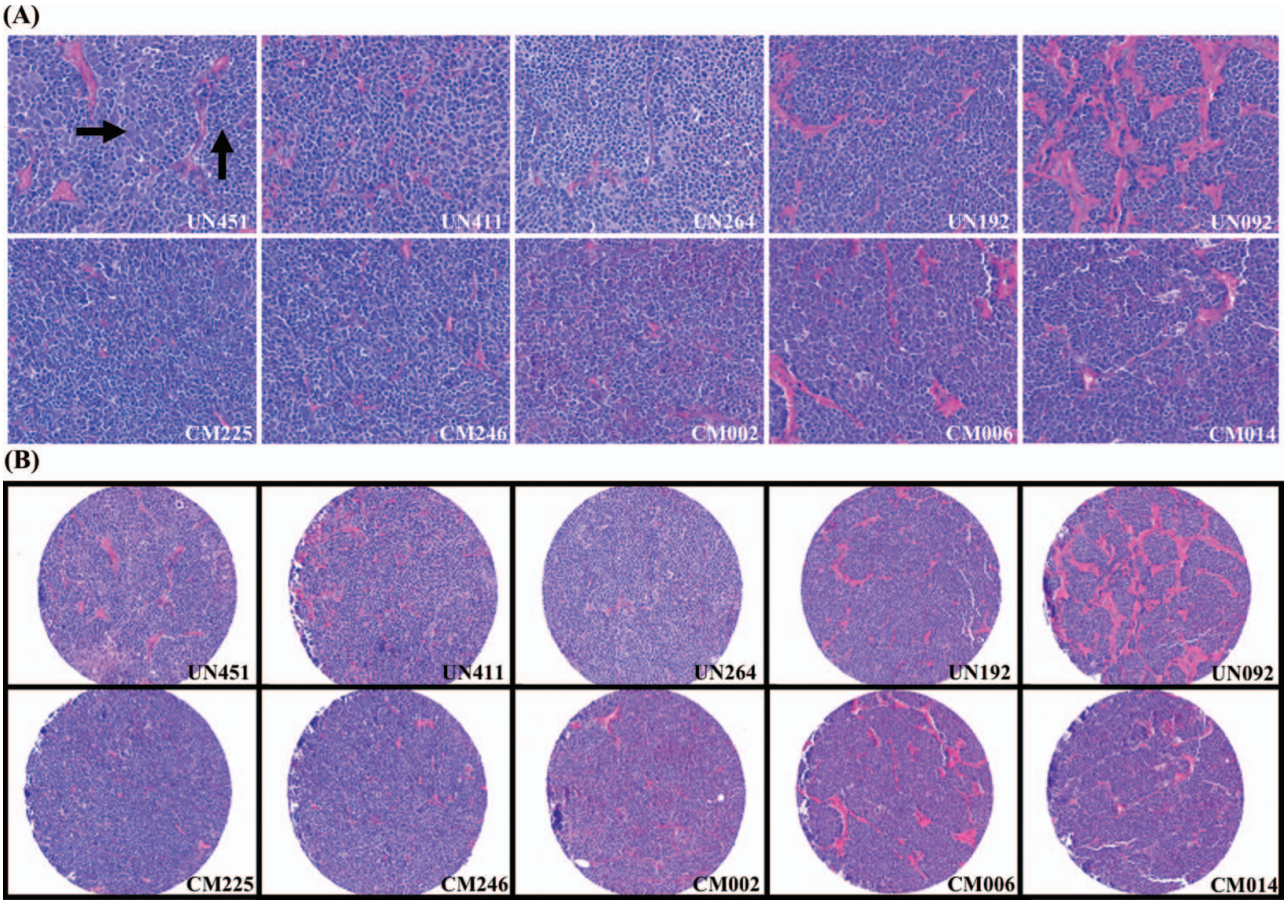

Figure 1. Imaging the histology of established orthotopic POB CM and POB UN series tumors utilizing a tumor tissue array. Transplantable POB CM and POB UN series neuroblastoma lines were established from spontaneous tumors arising in the MYCN transgenic mice with the 129svIMJ and C57BL6/J backgrounds, respectively, as described in "Materials and Methods" section. A tumor tissue array containing these tumors and matched normal tissues was constructed as described in "Materials and Methods" section, and then stained with hematoxylin and eosin. Panels (A) and (B) show 200× and 100× magnified views, respectively, of representative cores for each of the POB UN and POB CM series tumors. The sections demonstrate tumors consisting predominantly of small round blue cells with undifferentiated morphology and occasional larger differentiated cells in some tumors.

Cancer Invest Downloaded from informahealthcare.com by NIH Pathology Lab on 11/12/14
For personal use only.

RIGHTSLINK

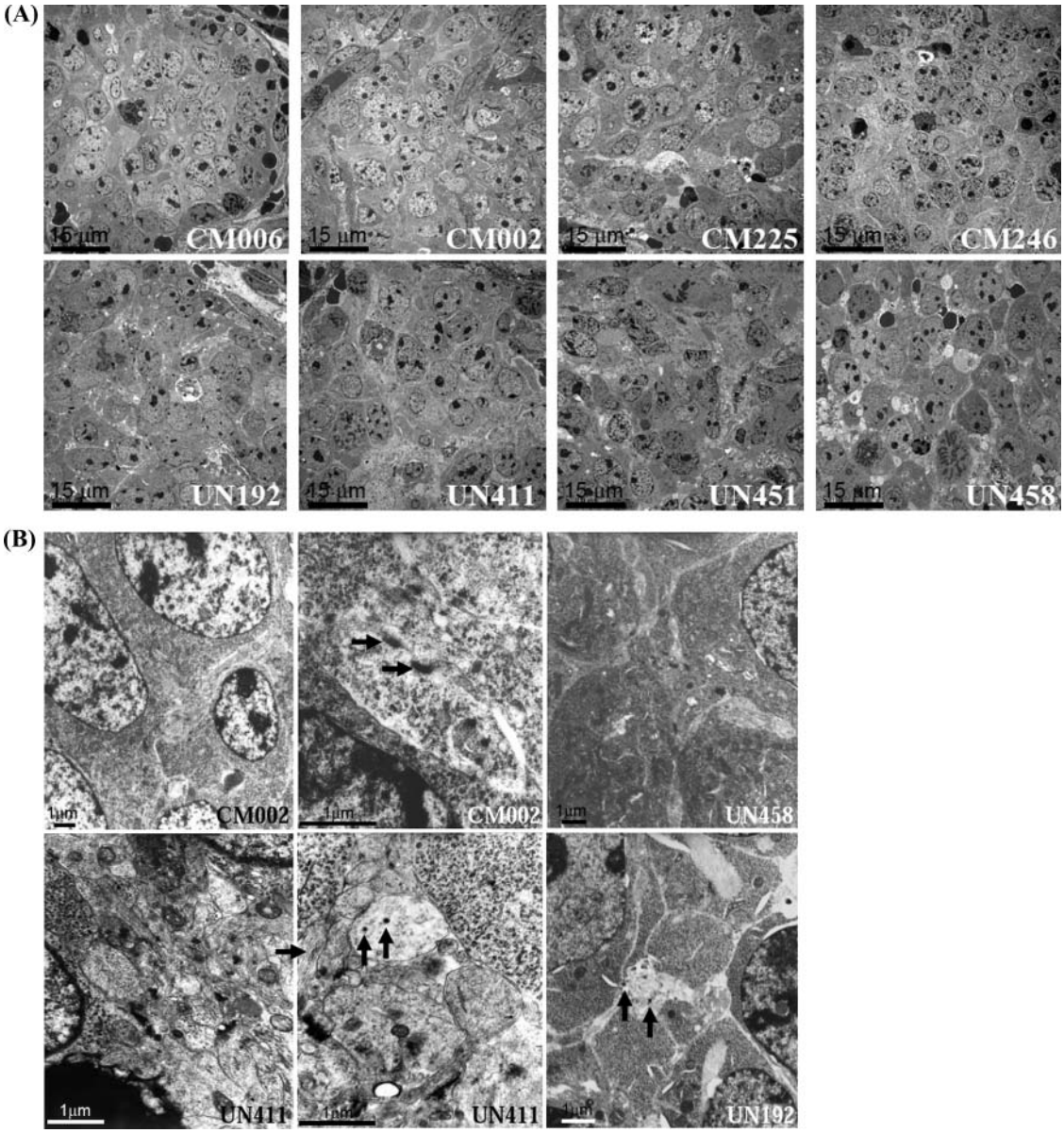

Figure 2. Ultrastructural histology of POB CM and POB UN series tumors imaged using transmission electron microscopy. Transplantable POB CM and POB UN series neuroblastoma lines were established from spontaneous tumors arising in the MYCN transgenic mice with the 129svIMJ and C57BL6/J backgrounds, respectively, as described in "Materials and Methods" section. Mice were euthanized by group and established tumors were resected and prepared for electron microscopy as described in "Materials and Methods" section. Representative images of the respective tumors were obtained at the indicated lower and higher magnifications, displayed in panels (A) and (B), respectively. In panel (B), characteristic neuroblastoma features are indicated as follows: in section CM002, the black arrows point to prominent intercellular attachments; section UN411 (bottom left) shows many cell processes. Two of these processes, shown at higher magnification (bottom middle), contain filaments (horizontal arrow), or dense core (neurosecretory) granules (vertical arrows). A cross-sectional process with dense core granules (vertical arrows) is also present in section UN192 (bottom right).

of predominantly undifferentiated tumor cells (Figure 1(A)), while others (CM225) were composed almost exclusively of undifferentiated tumor cell populations (Figure 1). Tissue arrays were also constructed using a panel of spontaneous neuroblastoma tumors resected from MYCN transgenic mice, and demonstrated similar histology overall (data not shown). Thus, both spontaneous MYCN transgenic tumors and transplantable tumors established utilizing POB CM and POB UN series cell lines demonstrate basic morphologic features most consistent with neuroblastoma, rather than ganglioneuroblastoma or ganglioneuroma.

Electron micrographic characterization of ultrastructural histology

We also utilized electron microscopy to investigate the ultrastructural histology of established orthotopic POB CM and POB UN series tumors. These tumors consist predominantly of undifferentiated round tumor cells with high nuclear:cytoplasmic ratio and frequent cytoplasmic glycogen, primitive attachments, and mitoses within the respective tumor specimens (Figure 2(A)). Some tumors exhibited neuroblastic differentiation, i.e., cell processes with or without filaments and neurosecretory granules (Figure 2(B)).

Cancer Invest Downloaded from informahealthcare.com by NIH Pathology Lab on 11/12/14
For personal use only.

RIGHTSLINK

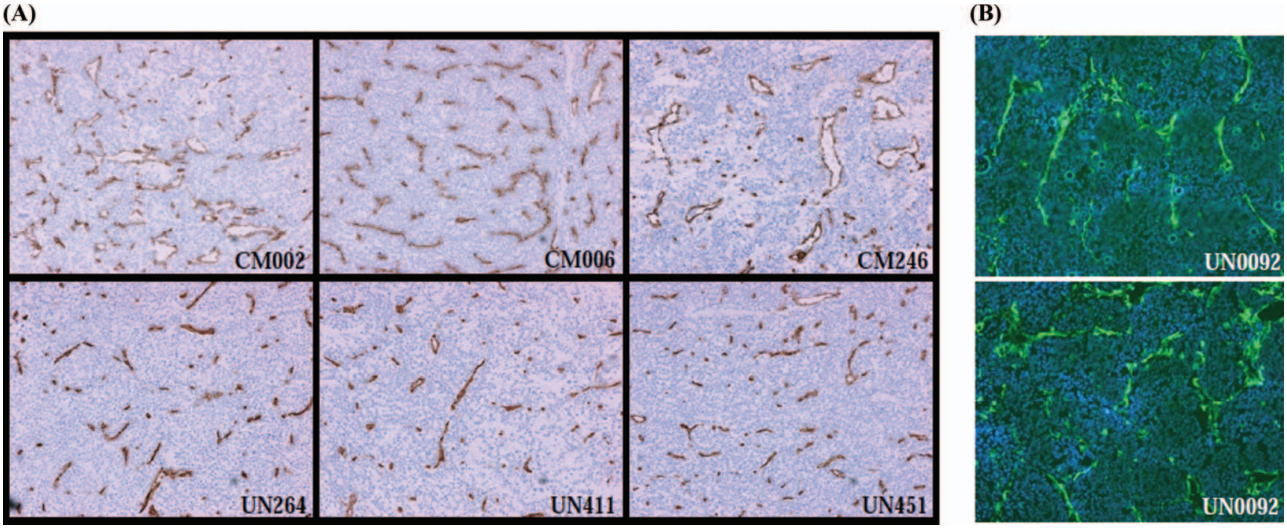

Figure 3. Vascularity of POB CM and POB UN series neuroblastoma tumors. Tumor specimens for each of the respective cell lines were processed and subjected to immunohistochemical staining for the vascular endothelial marker CD31 as described in "Materials and Methods" section. Tumor sections were imaged as described in "Materials and Methods" section, and representative fields are shown at 100× magnification [panel (A)]. The vascularity of these tumors was also demonstrated utilizing POB UN0092 tumor cells that were implanted subcutaneously in C57BL/6-TgN(ACTbEGFP)1Osb (actin GFP) mice as described in "Materials and Methods" section. At day 17 post implantation, POB UN0092 tumors were resected and processed for imaging via fluorescence microscopy as described in "Materials and Methods" section. Representative images are shown at 100× magnification [panel (B)]. Tumor sections were also stained with DAPI to demonstrate the morphology of nuclei in both the tumor and the endothelial cell compartments. The tumor vasculature within these sections is clearly delineated by the intense green fluorescence of endothelial cells lining these vessels. Both approaches demonstrate that POB CM and POB UN series neuroblastoma tumors are highly vascular.

Cancer Invest Downloaded from informahealthcare.com by NIH Pathology Lab on 11/12/14
For personal use only.

Investigation of tumor vascularity-CD31 immunohistochemistry/actin-GFP mice

Neuroblastoma tumors have been noted to be highly vascular in the clinical setting, with a propensity for intratumoral hemorrhage in some patients. In addition, increased tumor vascularity appears to correlate with more aggressive tumor growth, increased propensity for concurrent presence of metastasic disease, and adverse outcome in patients with advanced neuroblastoma (28). To evaluate the vascularity of both POB CM and POB UN series tumors, individual tumor sections were subjected to immunohistochemical staining for the vascular endothelial marker CD31 (Figure 3(A)). In addition, POB UN0092 cells were implanted into syngeneic actin-EGFP transgenic mice. These mice have been engineered to ubiquitously express GFP under the control of the actin promoter (15). As a consequence, tumor implants are vascularized by vessels that display intense expression of GFP. Vessel density within tumor sections can be readily visualized and imaged, and in conjunction with image analysis software, allows for direct quantitative analysis of tumor vascularization within tissue sections. Using immunohistochemical staining for CD31, we have found that both POB CM and POB UN series tumors are highly vascularized, consistent with human neuroblastoma tumors (Figure 3(A)). Further, implantation of POB UN series cell lines (UN0092) into actin-GFP mice leads to the formation of highly vascular tumors in which vascular density can be readily imaged with fluorescence microscopy and quantitated using image analysis software (Figure 3(B)).

Immunohistochemical assessment of neuronal markers

To investigate whether POB UN and POB CM series tumor specimens expressed various neuronal markers in a manner consistent with human neuroblastoma tumors, tissue arrays containing the respective tumor specimens were subjected to immunohistochemical staining as described in "Materials and Methods" section. Markers that were examined included neurofilament (NF), tyrosine hydroxylase (TH), synaptophysin (SYN), chromogranin (CRG), and neuron-specific enolase (NSE). Representative core sections for each tumor or matched control normal tissue sections from murine cerebral cortex and cerebellum were imaged at the indicated magnifications (Figure 4). All tumor specimens demonstrated a diffuse and intense pattern of immunohistochemical staining for neurofilament within the tumor microenvironment [Figure 4(C), 100 × magnification], while a distinct geographic pattern of differential staining was demonstrated in control tissue sections from the cerebral cortex (Figure 4(A)) and cerebellum [Figure 4(B)]. Variable expression of tyrosine hydroxylase (TH) was noted in the respective tumor specimens, and ranged from intense, diffuse expression of TH (CM0002, CM0014, UN0092, UN0451), intermediate intensity focal expression (CM0006, CM0246, UN0411), and lines that were essentially minimal to no expression [CM0225, UN0192, UN0264; Figure 4(D)]. Diffuse staining for synaptophysin was observed in all of the respective tumor cell lines, although the staining was much less intense than that observed with staining for either neurofilament or tyrosine hydroxylase (Figure 4(E)). Weakly positive diffuse staining

RIGHTSLINK

for chromogranin was noted in the respective cell lines (Figure 4(F)).

Profile of catecholamine production within local tumor site

Human neuroblastoma tumors commonly produce excess quantities of catecholamines, resulting in the presence of increased catecholamine levels in the serum and/or catecholamine metabolites in the urine (29, 30). Overproduction of catecholamines by neuroblastoma tumors can be utilized for diagnostic purposes in patients with neuroblastoma or for prospective monitoring of disease burden using urine or serum catecholamines as a disease marker. To investigate whether the respective POB CM and POB UN series tumors similarly overproduced catecholamines *in vivo*, the catecholamine content of these tumors was assayed as described in "Materials and Methods" section.

Notably, the respective neuroblastoma tumors were found to produce large quantities of norepinephrine, dopamine, and epinephrine, in particular, compared with either conventional murine neuroblastoma cell lines such as TBJ and Neuro-2a, nonneuroblastoma tumors such as orthotopic Renca murine renal cell carcinoma (Table 1), and normal tissues including liver, kidney, and adrenal gland. Much lower levels of catechols including DOPA, DOPAC, and DHPG were noted within these same tumor specimens. Notably, higher levels of norepinephrine and dopamine were observed in spontaneous tumors compared with the respective transplantable POB CM and POB UN series tumors (Table 1).

Microarray comparison by hierarchical clustering and principal component analysis

To provide a comprehensive profile of the patterns of gene expression within neuroblastoma tumors established utilizing the respective cell lines, snap-frozen specimens of both spontaneous and transplantable orthotopic intra-adrenal neuroblastoma tumors were prepared, and gene expression was evaluated using cDNA microarray as described in "Materials and Methods" section. Normal tissue specimens including syngeneic murine adrenal gland, heart, rib cage, lung, kidney, liver, brain, and spleen were used to provide a control expression profile for comparison. The relative similarity of the overall expression profiles for the respective tumor specimens and normal tissue specimens were compared utilizing hierarchical clustering (HC) and principal component analysis (PCA) as described in "Materials and Methods" section, and are shown graphically in Figures 5(A) and (B), respectively. Notably, both spontaneous tumors and transplantable POB CM and POB UN series tumors cluster in a pattern that is entirely distinct from normal tissues, including adrenal, heart, rib cage, lung, kidney, liver, brain, and spleen (Figure

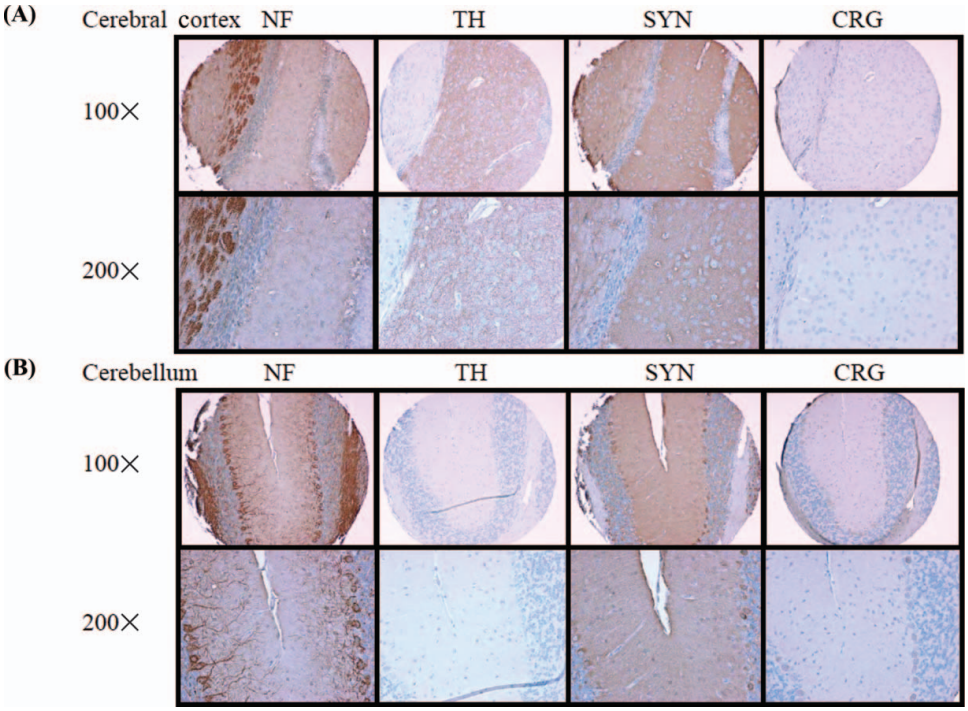

Figure 4. Expression of neuroblastoma-related tumor markers by POB CM and POB UN series tumors. Tumor tissue arrays containing POB CM and POB UN series tumors and matched normal control tissues were established as described in "Materials and Methods" section. These arrays were subjected to immunohistochemical staining for markers including neurofilament (NF), tyrosine hydroxylase (TH), synaptophysin (SYN), and chromogranin (CRG), and images of representative core sections (100× to 400× magnification where indicated) were obtained as described in "Materials and Methods" section. Sections of cerebral cortex and cerebellum display specific and geographic staining patterns for each of the respective markers at the indicated magnification [panels (A) and (B)]. Intense, diffuse expression of neurofilament [panel (C)] was noted in POB CM and POB UN series tumors, while tyrosine hydroxylase [panel (D)] displayed the greatest range of expression and patterning between tumors. Expression of synaptophysin [panel (E)] and chromogranin [panel (F)] was less intense than either neurofilament or tyrosine hydroxylase, but was present in all tumors.

Cancer Invest Downloaded from informahealthcare.com by NIH Pathology Lab on 11/12/14
For personal use only.

RIGHTSLINK

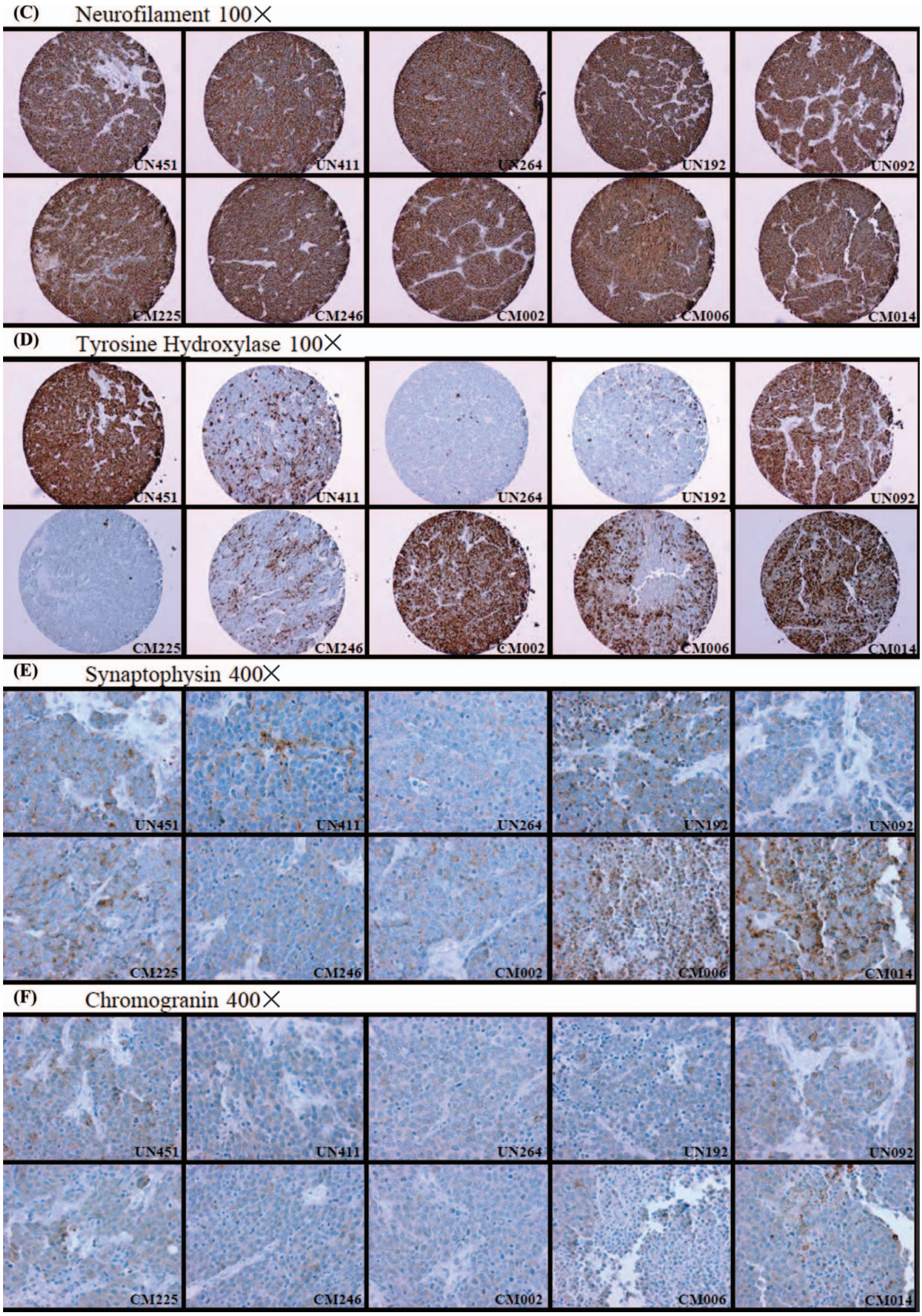

Figure 4. Continued.

Cancer Invest Downloaded from informahealthcare.com by NIH Pathology Lab on 11/12/14
For personal use only.

RIGHTSLINK

Table 1. Catecholamine content of murine neuroblastoma and tumor cell lines

	Tumor	DHPG (pg/mg)	NE (pg/mg)	DOPA (pg/mg)	EPI (pg/mg)	DA (pg/mg)	DQPAC (pg/mg)
Renca	Cell line	68	52	141	200	226	–
mi	Cell line	60	1, 805	646	191	279	–
TBJ	Cell line	102	1, 073	161	260	925	1, 042
CM002	Tumor line	–	16, 022	–	5, 352	1, 561	–
CM006	Tumor line	25	5, 372	53	567	1, 512	101
CM014	Tumor line	14	2, 489	46	423	1, 828	69
CM225	Tumor line	–	6, 770	–	4, 129	–	–
CM246	Tumor line	59	541	161	143	371	–
US092	Tumor line	68	8, 004	78	242	769	38
UN192	Tumor line	2	949	5	334	38	–
UH4I1	Tumor line	85	4, 121	148	167	658	–
US451	Tumor line	239	32, 446	157	316	3, 358	272
CM366	Spontaneous	113	27, 527	288	516	3, 766	–
CM620	Spontaneous	–	21, 107	100	533	3, 359	540
CM599	Spontaneous	4	1, 196	72	214	1, 804	28
UN151	Spontaneous	161	19, 708	104	218	997	228
Liver	Tissue	–	123	173	218	172	–
Kidney	Tissue	59	303	114	523	433	–
Adrenal gland	Tissue	648	219, 111	663	500, 670	7, 727	–

Notes: Catecholamine levels for DHPG, NE, DOPA, EPI, DA, and DOPAC were measured in 4 spontaneous neuroblastoma tumors, and in 5 tumor lines derived from the 129svIM/J (CM series) and 4 lines from the C57BL6/J strain (UN) series, as described in "Materials and Methods" section. For comparison, the TBJ and Neuro-2a neuroblastoma cell lines were analyzed, as were normal tissues (live, kidney, adrenal) and a renal carcinoma tumor line (Renca).

Cancer Invest Downloaded from informahealthcare.com by NIH Pathology Lab on 11/12/14
For personal use only.

5). More specifically, POB UN series tumors cluster together and are distinct from POB CM series tumors, while both series of transplantable tumors cluster distinctly from spontaneous POB CM series tumors and normal tissues. Thus, the analysis of global patterns of gene expression within these tumor specimens demonstrates that POB CM and POB UN series tumors are most similar to other tumors with the same background, and that the respective POB CM and POB UN series tumors demonstrate gene expression patterns that cluster distinctly from spontaneous tumors. A comprehensive summary of the specific genes evaluated by this microarray assessment and their patterns of expression within individual tumor specimens and normal tissue specimens can be accessed from an online database hosted by the Oncogenomics Section, POB, NCI-CCR (at http://pob.abcc.ncifcrf.gov/cgi-bin/JK).

Overexpression of selected genes in POB CM and POB UN series tumors

The respective expression profiles for orthotopic POB CM and POB UN series tumors were compared with a pooled expression profile for murine normal control tissues (Table 2). Using SAM analysis as described earlier, we identified a total of 3,705 differentially expressed genes, including 1,142 genes that were overexpressed twofold or more; and 2,563 genes that were underexpressed twofold or more compared with pooled normal control mouse tissues. A total of 30 selected genes of potential clinical utility that are highly expressed in POB CM and POB UN series tumors compared with normal tissues are shown in Table 2 (see http://pob.abcc.ncifcrf.gov/cgi-bin/JK for a full list of differentially expressed genes). Overexpressed genes include factors that have been shown to promote tumor neovascularization (*Robo/Slit2*) or inhibit apoptosis [survivin (*Birc5*), *Gsk3b*], and a large number of genes that play a critical role in cell cycle progression (including Aurora kinase, *Cdk4*, *Chek-1*, *Plk-1*, minichromosome maintenance genes, and cyclins A2, B1, B2, and D1). Other overexpressed genes of interest include immune-modulating genes such as macrophage migration inhibitory factor (*Mif*) and *B7h3*, neurofilament (immunohistochemical marker found to be overexpressed by POB CM and POB UN series neuroblastoma tumors) and several other potential therapeutic targets including *Hdac2*, nucleolin, nucleophosmin, topoisomerase 2a, and *Uch11*.

Downregulation of selected genes in POB CM and POB UN series tumors

Compared with the expression profile of pooled normal tissues, established POB CM and POB UN series tumors demonstrate downregulation in the expression of several physiologically relevant genes known to inhibit tumor neovascularization or induce tumor cell apoptosis, tumor suppressors, metastasis suppressors, and genes that mediate the responsiveness of tumor cells to the host immune response (Table 3). Antiangiogenic genes including *Tipm2* and *Timp3*, *Timp4*, *Cd47* (thrombospondin receptor), and *Zfp36l1* were downregulated in these tumors compared with control tissues, as were several genes capable of mediating apoptosis including annexin A5, *Birc3*, *Bnip3/Bnip3* ligand, caspases 6 and 12, clusterin, *Dap*, *Foxo1*, *Gas1*, *Igf1*, lymphotoxin beta receptor, and *Pten*. In addition, the expression of metastasis suppressor genes including CD9, cystatin C, cadherins 1 and 5, decorin, and *Kai1* was reduced, as were tumor suppressor genes including *Dab2*, *Dkk3*, *Lats2*, *Ndrg2*, scotin, *Tgfbr2*, *Wnt-4*, and *Wnt-5a.* Lastly, a substantial reduction of CD44 was noted in POB CM and POB UN series tumors compared with normal control tissues, as were several genes encoding mediators of cellular responses to IFN-γ, including the IFN-γ receptor as well as *Stat-1*, *Stat-3*, and *Jak-1*.

RIGHTSLINK

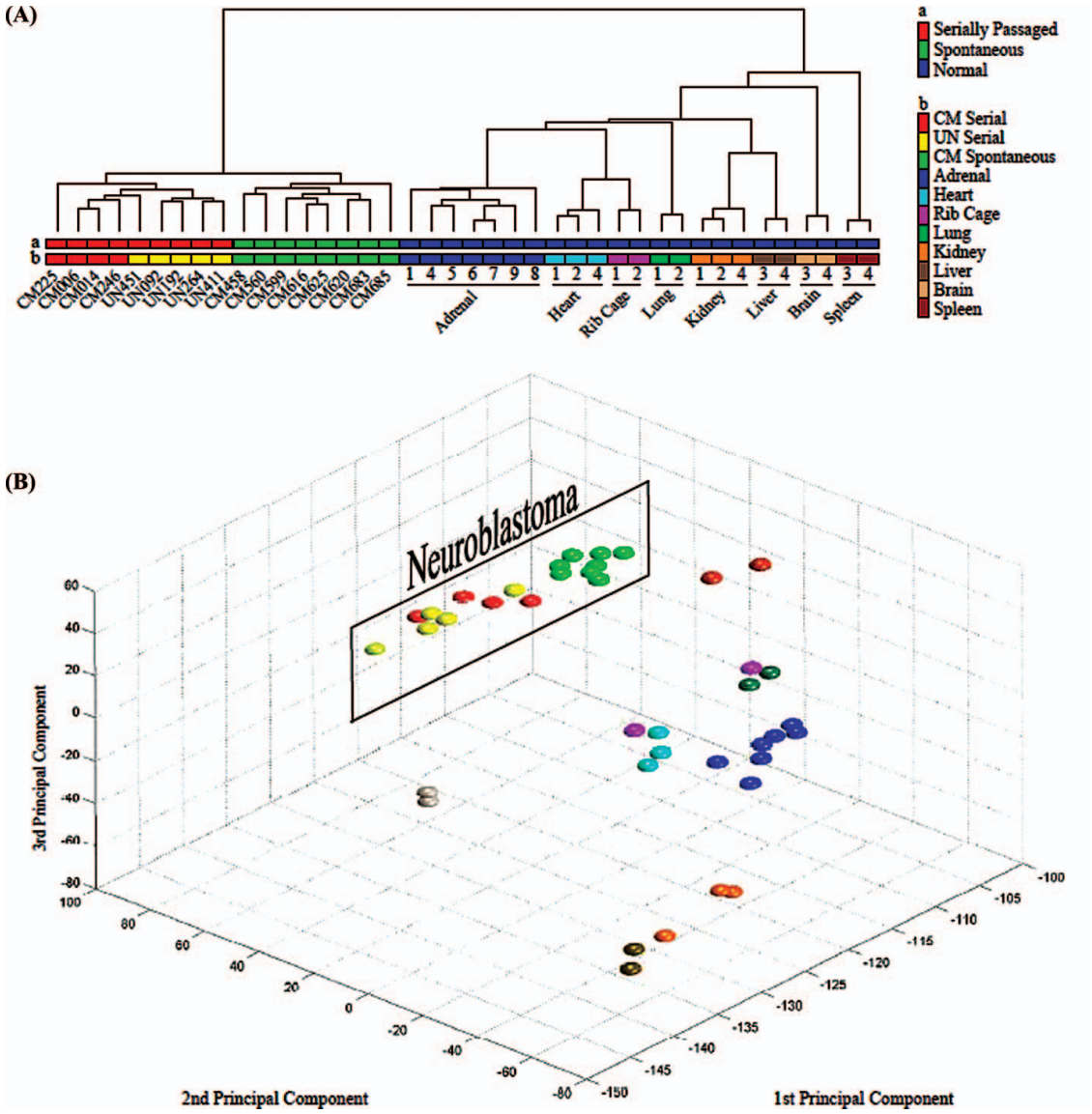

Figure 5. Hierarchical clustering and principle component analysis of the gene expression profiles of POB CM and POB UN series tumors and matched normal tissues. The patterns of gene expression within spontaneous MYCN transgenic tumors, established POB CM and POB UN series tumors, and matched normal control tissues were determined utilizing cDNA microarray as described in "Materials and Methods" section. These gene expression profiles were compared using both hierarchical clustering [HC; panel (A)] as well as principal component analysis [PCA; panel (B)]. The global relatedness of the respective expression profiles can be graphically represented by their arrangement in a dendrogram [hierarchical clustering, panel (A)] or by their positions in a three-dimensional space [principle component analysis, panel (B)]. These analyses demonstrate a close correspondence in the global expression profile of these tumors, with tumors segregating that are distinct from normal tissues, and spontaneous tumors clustering that are distinct from the respective POB CM and POB UN series tumors.

Cancer Invest Downloaded from informahealthcare.com by NIH Pathology Lab on 11/12/14
For personal use only.

Confirmation of selected differentially expressed genes in POB CM and POB UN series tumors

To confirm the differential expression of genes detected by microarrays, we performed quantitative RT-PCR on a set of 11 genes including 8 that were upregulated (*Aura*, *Birc5*, *Ccnd1*, *Cdk4*, *Chek1*, *Mcm2*, *Plk1*, and *Slit2*), 2 that were downregulated (*Clu* and *Foxo1*), and a housekeeping gene (*GAPDH*). We confirmed the significant differential expression, and as expected, the fold change in the differential expression was significantly larger by qRT-PCR than microarrays (Figure 6).

Cdk4 immunohistochemistry

We subsequently interrogated the POB CM and POB UN series tissue arrays to validate the local expression of Cdk4 protein, a key cell cycle gene that was found to be strongly overexpressed in the POB CM and POB UN series tumors using cDNA microarray. Notably, a significant expression of Cdk4 protein was noted within all tumors in the tissue array using immunohistochemical staining (Figure 7), confirming the utility of these tissue arrays for validation of the expression of potential therapeutic targets within POB CM and POB UN series tumors.

RIGHTSLINK

Table 2. Unregulated genes in POB neuroblastoma tumor line RNA microarray analysis

Category	Encoded protein, symbol	Image clone	Fold increase
Angiogenesis	Robol	BG078518	3.2
	Slit2	615062	6.4
Apoptosis	Survivin, Birc5	BG077309	3.9
	Gsk3b	BGK3622	2.5
Cell cycle	Aurora kinase, Aurka	BG077290	4.5
	Cdc25a	BGC80167	4
	Cdca7	BG064984	3.1
	Cdk4	BG087999, BG085009	4.2–4.6
	Chek1	BG070939, AU022576	4.2–4.3
	CydinA2, Ccna2	BG073518	4.1
	CydinB1, Ccnb1	BG078426, 634707, BG071965	4.2–6.2
	CydinB2, Ccnb2	BG071915	2.3
	CydinD2, Ccnd1	BGC83088	5.1
	Ezh2	634864, BG074931	2.5–2.9
	Mcm2	BG074668	3.8
	Mcm3	BG065055	3.7
	Mcm5	BG064865	4
	Mcm6	BG075357	4.4
	Mcm7	BG074721	3.9
	Plk1	BG078368	5.1
High-mobility group proteins	Hmgb1	BG075297, BG086426	2.6–3.1
	Hmgb2	BGC85427	4.2
Immune	Mif	BG077749	3.7
	B7h3	BGC83832	2.1
Miscellaneous	Baspl	BG064661	6.6
	Hdac2	BG086215	2.4
	Neurofilament, NefI	AU043877	9.9
	Nucleolin, Ncl	BG077519, AW541474, BG064932	3.6–4.7
	Nucleophosmin, Npml	BG074521, BG074522	4.4–4.9
	Top2a	BG079172, BG087390	5.1–5.3
	Uchll	BG067910, BG086722	7.2–8.8

In vivo growth characteristics and survival after IA, IV, or IS tumor cell implantation

As described earlier, we performed studies to compare the *in vivo* growth characteristics of the respective POB CM and POB UN series cell lines after orthotopic intra-adrenal implantation, and the formation of induced metastases after the injection of these lines either intravenously (IV) or intrasplenically (IS) (Table 4). Injection of 2×10^5 cells orthotopically in the adrenal gland results in median survival times ranging from 20 to 44 days for POB CM series lines and from 35 to 57 days for POB UN series lines. In these mice, the time to 100% lethality ranged from 22 to 49 days for POB CM series cell lines and from 45 to 81 days for POB UN series cell lines. Further, injection of 2×10^5 tumor cells intravenously or intrasplenically results in the formation of metastases in the livers of mice injected with 4 of the 5 POB CM series cell lines versus 1 of 4 POB UN series cell lines. Collectively, these studies demonstrate that POB CM and POB UN series cell lines can be implanted to form primary and/or metastatic tumors in syngeneic mice, and suggest that POB CM series tumors may behave somewhat more aggressively than POB UN series tumors.

DISCUSSION

The prognosis of patients with high-risk neuroblastoma is guarded despite conventional therapy that incorporates surgery, radiotherapy, combination chemotherapy, autologous stem cell transplantation, differentiating agents, and immune therapy (31, 32). Patients with high-risk neuroblastoma are prone to relapse, and a subset of patients with particularly poor prognosis may nonetheless be refractory to this aggressive "up-front" approach to therapy. There remains an urgent need then to identify new therapeutic approaches for patients with advanced neuroblastoma. Toward this end, the present studies now describe a panel of novel transplantable neuroblastoma tumor cell lines that we have derived from spontaneous tumors in MYCN transgenic mice. Existing preclinical studies have emphasized the use of xenograft models in which human neuroblastoma cell lines are transplanted into immunodeficient mice or syngeneic models that utilize murine neuroblastoma cell lines including Neuro-2a, TBJ, and NSX2 (5). More recently, a unique transgenic mouse model has been developed, in which tissue-specific overexpression of MYCN under the control of a tyrosine hydroxylase promoter results in the development of spontaneous neuroblastoma tumors in the adrenal gland and the paraspinal sympathetic chain ganglia (14). Spontaneous neuroblastoma tumors arise in these mice between 2 and 3 months of age, with substantial differences in tumor penetrance noted among the respective strains (14). In mice with the 129svIM/J background, virtually 100% tumor penetrance is noted, while much lower tumor penetrance is noted for MYCN transgenic mice with the C57BL/6J background (unpublished observation). Using this model, new therapeutic agents can be investigated in a tumor-bearing host that has

Cancer Invest Downloaded from informahealthcare.com by NIH Pathology Lab on 11/12/14
For personal use only.

RIGHTSLINK

Table 3. Downregulated genes in POB neuroblastoma tumor line RNA microarray analysis

Category	Encoded protein, symbol	Image clone	Fold decrease
Angiogenesis	Cd47	598502	5.3
	Timp2	BG0S8451	4
	Timp3	BG0S5154, BG055466	4.8–16.7
	Timp4	BG0S4374	5.6
	Zfp3611	BG0S6598.598609	9.1–11.1
Apoptosis	Annenn A5, Anxa5	BG077508	2.8
	Ba-c3	BG0S44O5, BGOS9214	2.1–2.6
	Bnip3	BGOS7162	6.3
	Bnip3L	AW556222	2.4
	Caspase-6, Casp6	475851, BG076240	2.6–4.0
	Caspase-12, Caspl2	BG0S6S81	3
	Chusterin, Chu	BG072209	12.5
	Dap	BG0S4087	3.8
	Gasl	BGOS7671	3.6
	Giiml9	40S866, BG0S6273	2.2–2.6
	Lvmphotoxin beta R	BG067106	4.2
	Nftbl	BG0S2106	3.3
	Pten	619291, BGCS3236	3.2–3.6
Immune response	B2-microglobulin, B2m	BG063994.596438	4.0–5.3
	Ifngr2	576679	2.2
	Jakl	BGCS7301, BG067S74	3.1–4.2
	Jak2	BG0S1632	2.9
	Stat-l	577484	2.9
	Stat-3	BGO84377, BG076355	3.1–4.2
	Stat-4	577343	3
	Interieukn-18, II18	BG088827	6.7
	Jam2	BG072316, BG07083	3–4.8
Metastasis suppressors	Alpha-catemn 1, Catnal	BG077688, BG066669, BG080026	2.2–5.0
	Cadherin-1, Cdhl	605280	4.5
	Cadherin-5, Cdh5	385761, BG077522	2.2–2.5
	Decorin, Dcn	BG0S8078, BG086986	4.6–5.6
	Kail	BG0S8538, BG087428	2.7–7.7
	Cd9	BG0S7410	5.9
	Cystatm C, Cst3	BG078926	5.3
Tumor suppressors	Dab2	BG085400.599270, BG054928	4.2–11.1
	Dkk3	BG0S8107	3.8
	Klf4	BG064062, BG069413	4.2–10.0
	Lats2	BG072604	10
	Ndrg2	349612	10
	Scotim	BG074542	9.1
	TGfbr2	BG0S5088	5.3
	Wnt4	BG0S6084	2
	Wnt5a	600775	3.7
Miscellaneous	Cd44	BG068522	5.3
	Foxol	BG068406, BG084378	5.6–10.0
	Foxo3	BG065768.621038	2.7–2.8
	Idb3	AW557873	5.6
	Igfl	BG075165	7.1
	Mxd4	BG074125	5.6

been conditioned by the complete dynamic process of neoplastic progression and tumorigenesis. Nonetheless, variability in the timing for tumor development limits the practical utility of this model for therapy studies or studies to investigate the mechanisms of action by new therapeutic agents. To expand the utility of the MYCN transgenic mouse model, the present report describes a panel of novel transplantable cell lines that we have derived from spontaneous MYCN transgenic neuroblastoma tumors, and studies to characterize the histopathologic and molecular features of tumors established using these respective POB CM and POB UN series cell lines.

To provide a high-throughput tool for the investigation of the microenvironment of orthotopic POB CM and POB UN series tumors, we have now constructed tissue arrays containing these tumors as well as paired normal control tissues including the adrenal, brain, liver, lung, kidney, heart, and spleen. This represents the first use to our knowledge of tissue array technology for investigation of the biology of neuroblastoma tumors. Evaluation of the histopathologic features of these tumors demonstrates that they possess a range of characteristics that are consistent with human neuroblastoma tumors. Staining of the tissue array with hematoxylin and eosin reveals that POB CM and POB UN series neuroblastoma tumors are highly vascular with a predominance of relatively undifferentiated small round blue cells, accompanied in some tumors by more differentiated cells characteristic

Cancer Invest Downloaded from informahealthcare.com by NIH Pathology Lab on 11/12/14
For personal use only.

RIGHTSLINK

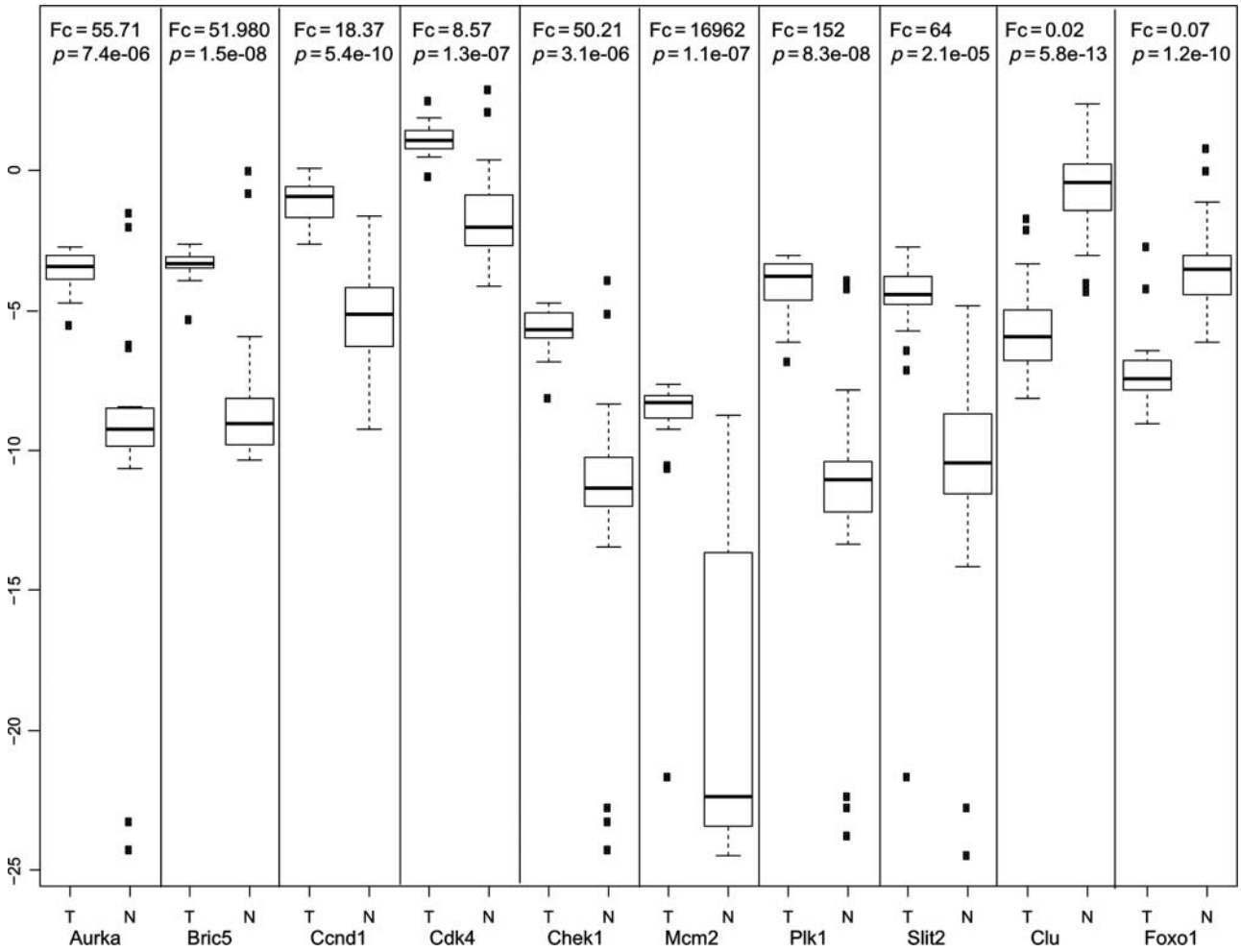

Figure 6. Taqman assays validate the results from microarray experiments. Box plots were used to demonstrate the expression levels of indicated genes in tumor samples (T, $n = 24$) and normal mouse tissues (N, $n = 23$). Expression level of each gene is represented by $-\delta$Ct ($Ct_{gene} - Ct_{GAPDH}$). The middle thick lines in box plots are medians, and the dots represent outliers. Fc represents fold change that was calculated as $2^{-\delta\delta Ct}$ using median δCt for tumor ($n = 24$) or normal tissue ($n = 23$) groups and p values were determined by the Welch's t-test.

of ganglion cells. In addition, variability in the relative stromal content was observed across the different tumors, as has been noted in the clinical setting (33). Although subsequent electron micrographic studies confirmed the predominantly undifferentiated morphology of POB CM and POB UN series tumor cells, these studies have also confirmed the presence of neurosecretory granules, neuritic processes, and neuropil within these tumors. Immunohistochemical staining of tumor tissue arrays further demonstrates that POB CM and POB UN series tumors also express several markers that are commonly observed in human neuroblastoma tumors (1), including neurofilament, chromogranin, tyrosine hydroxylase, and, to a lesser degree, synaptophysin. Collectively, these observations indicate that POB CM and POB UN series tumors possess many of the histopathologic features observed in both human neuroblastoma tumors (33, 34) and spontaneous tumors that arise in MYCN transgenic mice (14).

To investigate the biochemical similarity of POB CM and POB UN series cell lines to human neuroblastoma tumors, we subsequently profiled patterns of catecholamine production within these tumors. The production of large quantities of catecholamines is a common feature of the majority of human neuroblastoma tumors, and an assay of catecholamine levels in the serum (norepinephrine, epinephrine, dopamine) and/or urine (homovanillic acid-HVA, vanillymandelic acid-VMA) of patients with neuroblastoma is used both for diagnostic purposes at the time of presentation and as a tumor marker that provides an indirect measure of disease burden during therapy (35, 36). Looking at patterns of catecholamine production directly within the tumor microenvironment, we observed a marked overproduction of NE, EPI, and dopamine both within spontaneous tumors from MYCN transgenic mice and the respective POB CM and POB UN series tumors. Levels of DOPA and DA seemed to be somewhat less in tumor lines as compared with spontaneous tumors, while the levels of DHPG varied widely. Notably, the levels of catecholamine production within these tumors far exceed what is observed both within established non-neuroblastoma tumors such as Renca murine renal cell carcinoma or normal tissue. Levels in the murine neuroblastoma cell lines TBJ and Neuro-2a fell within the range of variability seen in

Cancer Invest Downloaded from informahealthcare.com by NIH Pathology Lab on 11/12/14
For personal use only.

RIGHTSLINK

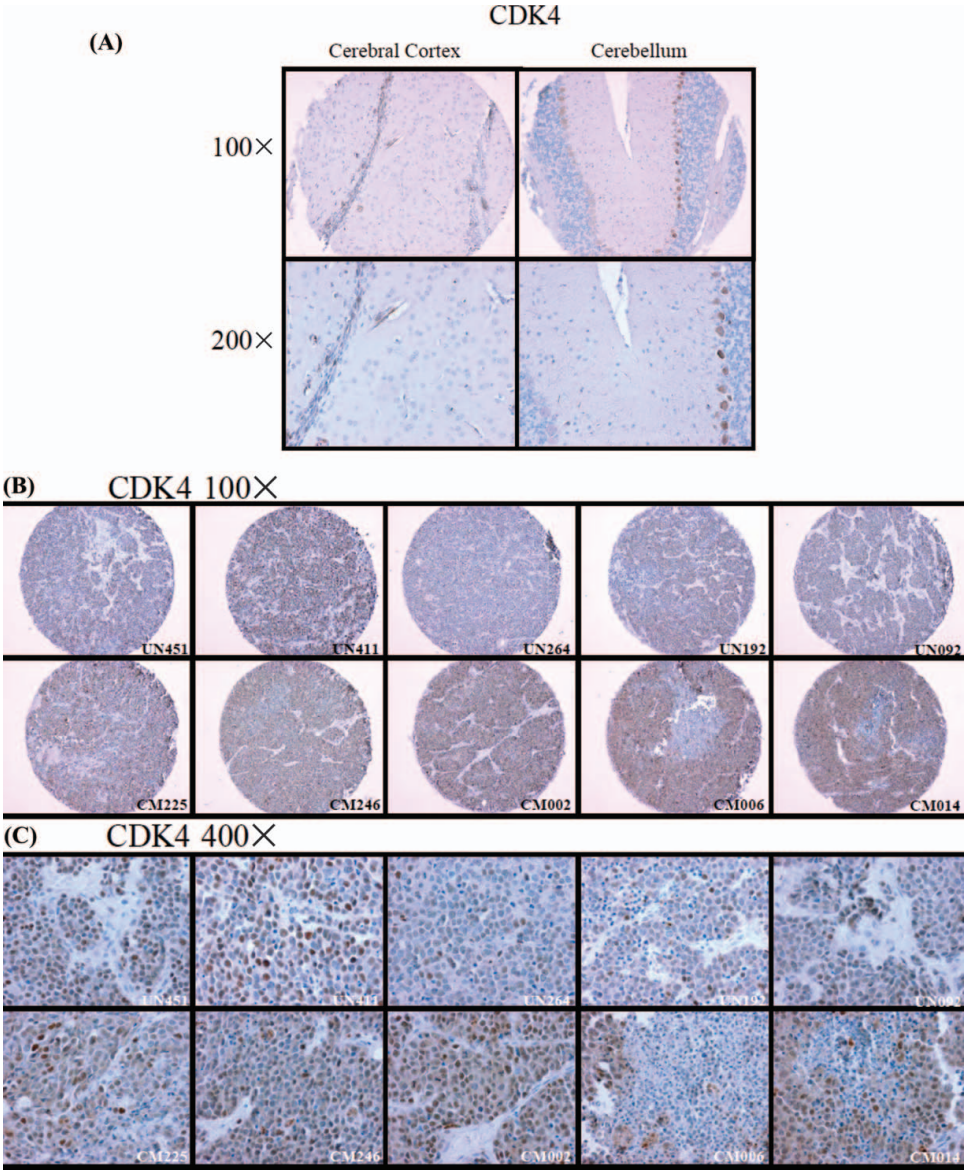

Figure 7. Expression of Cdk4 protein within the local microenvironment of POB CM and POB UN series tumors. Tumor tissue arrays containing POB CM and POB UN series tumors and matched normal control tissues were established as described in "Materials and Methods" section. This array was subjected to immunohistochemical staining for Cdk4 to confirm the expression of Cdk4 protein within the microenvironment of POB CM and POB UN series tumors, and representative tumor and normal tissue cores were imaged as described in "Materials and Methods" section. Specific geographic expression of Cdk4 protein is noted within the cerebral cortex and cerebellum [panel (A), 100× and 200× magnification], while Cdk4 expression in representative sections of POB CM and POB UN series tumors is shown at 100× [panel (B)] and 400× [panel (C)] magnification, respectively. Cdk4 expression is noted in the majority of POB CM and POB UN series tumor cells.

spontaneous and tumor lines. The variation seen in the spontaneous tumors alone indicates that catecholmine biosythesis is often amplified, but is not a uniform hallmark of transformation.

The present report provides the first description to our knowledge of the expression profile for murine neuroblastoma tumors that arise in MYCN transgenic mice. These observations further confirm the close correspondence between POB CM and POB UN series tumors and biologic features noted in human neuroblastoma tumors. Using a 13,958 gene cDNA microarray chip, we have identified a close correspondence in the pattern of gene expression within established orthotopic POB CM and POB UN series tumors. Further, although both hierarchical clustering and principal component analysis indicate that established POB CM and POB UN series tumors cluster distinctly from spontaneous tumors, the differences between them were relatively modest, and all tumor specimens cluster distinctly from normal organs including adrenal, heart, lung, kidney, liver, and spleen. Of interest, in future studies, would be to compare the expression profile of the spontaneous and passaged tumor lines with *in vitro* cultured lines. Although the primary purpose of this report is to develop serially transplantable cell lines for murine neuroblastoma, we have been able to culture some of the serially passaged lines *in vitro* (data not shown). As expected, the spontaneous tumors clustered separately from the

Cancer Invest Downloaded from informahealthcare.com by NIH Pathology Lab on 11/12/14
For personal use only.

RIGHTSLINK

Table 4. Survival and lethality times for mice orthotopically (IA) implanted with POB neuroblastoma lines. Hepatic metastatic burden also provided for respective lines disseminated by IV or IS injection

	LA (2×10^5 cells)			
Tumor line	Median survival (days)	100% Lethality (days)	IV (2×10^5 cells) Hepatic mets[b]	IS (2.5×10^5 cells) Hepatic mets[b]
UN092	35, $n = 10$	47, $n = 10$	0	0
UN192	38, $n = 10$	45, $n = 10$	++++	++++
UN264	44, $n = 10$	59, $n = 10$	0	0
UN451	57, $n = 10$	81, $n = 9$[a]	0	0
CM002	20, $n = 10$	34, $n = 7$[a]	0	+
CM006	22, $n = 10$	22, $n = 10$	0	0
CM014	27, $n = 10$	29, $n = 10$	+	+
CM225	44, $n = 10$	49, $n = 10$	++++	++++
CM246	39, $n = 10$	49, $n = 10$	++++	++++

Notes: *In vitro* growth and survival characteristics. The POB UN and POB CM series of tumors listed were administered to groups of 10 mice orthotopically (IA, inter-adrenal), and median survival and 100% lethality recorded in days. These same lines were also administered intravenously (IV) or intrasplenically (IS) and analyzed for the presence of liver metastases as indicated prior to mice becoming moribund, as described in "Materials and Methods" section.
[a]Animals censored from analysis for nontumor-related reasons.
[b]Hepatic metastatic burden graded as follows: 0, none; +, 10%–20%; ++, 20%–50%; +++, 50%–90%; and ++++, 90%–100% livers displaying metastasis.

Cancer Invest Downloaded from informahealthcare.com by NIH Pathology Lab on 11/12/14
For personal use only.

serially passaged lines, although the difference is modest based on the hierarchal clustering distance shown in Figure 5(A). Given that we have not passaged these lines over a period of years, we recommend that, prior to extensive experimental use, cells be viably frozen into multiple early passage aliquots. Further, as described in more detail in the following sections, we found that POB CM and POB UN series tumors express high levels of several genes that have been associated with the pathobiology of neuroblastoma tumors and/or genes that represent potential targets for the treatment of neuroblastoma.

Angiogenesis genes

Human neuroblastomas are well recognized to be highly vascular tumors in the clinical setting, and previous studies suggest that the increased tumor vascularity can correlate with adverse outcome in patients with advanced neuroblastoma (28). These observations have fueled intense interest in the mechanisms that regulate the vascularization of neuroblastoma tumors (37–39). More recent studies have now shown that interaction between Slit2 and its receptor Robo1 may play an important role in regulating the vascularization of melanoma tumors (40), another tumor that arises in cell populations that are derived from the neural crest. A total of three Slit family genes have been described (41), with these genes playing a clear role in regulating both axonal guidance and neuronal migration (42, 43). Robo is a transmembrane protein and includes four distinct family members (41). Several-fold increases in the expression of genes encoding both *Robo1* and *Slit2* were observed within POB CM and POB UN series tumors. Recent studies have also demonstrated that *Robo2* appears to be overexpressed in poor prognosis human neuroblastoma tumors and increased *Slit3* expression can be observed in good prognosis neuroblastoma tumors (25). Although the role of Robo and Slit family members in regulating the neovascularization and/or metastatic spread of neuroblastoma tumors remains to be defined, our observations indicate that the role of this pathway in neuroblastoma tumors *in vivo* may be investigated using POB CM and POB UN series tumors.

We also observed marked reductions in the expression of the gene encoding CD47, a receptor for thrombospondin-1 (*Tsp-1*) (44). Thrombospondin-1 is a potent inhibitor of tumor neovascularization (45), and gene methylation with reduced expression of TSP-1 has been described in human neuroblastoma cell lines (46). Retinoic acid can induce cellular differentiation and the production of thrombospondin-1 by neuroblastoma tumor cells, and thrombospondin-1 mediates the ability of retinoic acid to induce this differentiation (47). In turn, forced expression of CD47 in neuroblastoma tumor cell lines has been shown to promote cellular differentiation *in vitro*, including the formation of neurite extensions (48). Thus, several lines of evidence suggest that reduced expression of CD47 and signals mediated by interactions between thrombospondin-1 and CD47 could contribute to the pathophysiology of neuroblastoma tumors. In turn, POB CM and POB UN series tumors may provide a useful model system for investigation of the role of thrombospondin-1 and CD47 interaction in regulating the biology of neuroblastoma tumors.

We have also noted marked reductions in the expression of genes encoding the antiangiogenic mediators *Timp2*, *Timp3*, and *Timp4* within POB CM and POB UN series tumors. TIMP molecules can suppress tumor neovascularization and appear to exert their effects via inhibition of the function of proangiogenic matrix metalloproteinases (49, 50). Reduced expression of TIMP molecules has been noted in human neuroblastoma cell lines and/or tumor specimens (51), and constitutive overexpression or retrovirus-mediated delivery of the TIMP genes can inhibit the vascularization and growth of murine neuroblastoma tumors *in vivo* (52, 53). In light of their low levels of TIMP expression and ability to form highly vascular tumors, POB CM and POB UN series tumors may be well suited for investigating the biologic and therapeutic effects of TIMP replacement therapy for neuroblastoma.

Apoptosis genes

Neuroblastoma tumor may possess a range of molecular alterations that may confer a resistance to apoptosis

RIGHTSLINK

Cancer Invest Downloaded from informahealthcare.com by NIH Pathology Lab on 11/12/14
For personal use only.

including the loss and/or silencing of proapoptotic genes such as caspases (54, 55), death receptors including FAS (56) and TRAIL-R (46), as well as overexpression of prosurvival factors including survivin (57, 58), Bcl-2 (59), Flip (60), and Akt (61, 62). There has been a significant interest in the role of survivin, a key antiapoptotic protein, both in the pathophysiology of neuroblastoma (57, 58) and as a potential therapeutic target for neuroblastoma (63, 64). Survivin maps to chromosome 17q25 (58), a region for which chromosomal gains are commonly noted in advanced neuroblastomas (65, 66). Survivin is downregulated in cells induced to undergo apoptosis by retinoic acid (67), an important agent in the therapy of patients with high-risk neuroblastoma (31). In turn, transfection of cells to overexpress survivin enhances their resistance to apoptosis induced by retinoic acid *in vitro* (58). The efficiency of survivin in enabling tumor cells to resist apoptosis has focused attention on efforts to therapeutically target survivin by utilizing approaches that include small molecules, siRNA, and tumor vaccination (68, 69). Our observations indicate that POB CM and POB UN series tumors express high levels of survivin and, thus, may be particularly well suited for preclinical investigation of the mechanistic role of survivin within neuroblastoma tumors, and approaches to therapeutically target this pathway *in vivo*.

Cell cycle genes

POB CM and POB UN series tumors also overexpress several genes that play an important role in cell cycle progression, including Aurora kinase A, *Cdk4*, *Chek-1*, *Plk-1*, minichromosome maintenance genes, and cyclins A2, B1, B2 and D2. Further, using immunohistochemical staining, we have confirmed the expression of Cdk4 protein within POB CM and POB UN series tumors, and demonstrated the use of tissue arrays for high-throughput validation of the expression of target genes at the protein level within the microenvironment of neuroblastoma tumors. The relative role of these respective genes in the pathogenesis of spontaneous tumors that arise in MYCN transgenic mice, and the POB CM and POB UN series cell lines that we have derived from these tumors remains to be defined. Nonetheless, several of these cell cycle genes represent potential therapeutic targets for neuroblastoma that can now be directly evaluated using POB CM and POB UN series tumors. More specifically, new therapeutic agents that target cell cycle regulators including Aurora kinase (70, 71), Cdk4 (72), Chek-1 (73), Plk-1 (74, 75), and cyclins (76, 77) have been developed and may warrant investigation in this preclinical model of advanced neuroblastoma.

Metastasis and tumor suppressor genes

Although their role in the biology of POB CM and POB UN series tumors remains to be defined, our present studies have demonstrated significant decreases in the expression of several genes with recognized activity as suppressors of tumor metastasis, including Kai1 (78), cadherin and catenin family members (cadherins-1, cadherin-5, alpha-catenin-1) (79–81), decorin (82), CD9 (83), and cystatin C (84). Among these genes, the low-level expression of Kai1 (85) has also been described in human neuroblastoma tumors. Decreased expression of several genes with reported tumor suppressor activity was noted as well within POB CM and POB UN series tumors, including Dab2 (86), Dkk3 (87), Klf4 (88), Lats2 (89), Ndrg2 (90), scotin (91, 92), and Wnt family members such as Wnt4 and Wnt5a (93, 94). Among these genes, reduced expression of Wnt-5a has recently been described in human neuroblastoma tumors and cell lines, and treatment with retinoic acid can increase the expression of Wnt-5a *in vitro* (95). The respective POB CM and POB UN series tumors may provide a useful model system then for investigating the impact of direct replacement of these genes on tumor pathophysiology or the antitumor efficacy of novel agents capable of modulating the expression of these genes within POB CM and POB UN series tumors *in vivo*.

Immune response genes

Interferon-γ (IFN-γ) plays a central role in mediating endogenous immune surveillance mechanisms that regulate tumor growth *in vivo* (96), and is an important downstream effector pathway for potent antitumor cytokines including IL-12 (97), IL-18 (98), and IL-27 (99). In turn, IFN-γ acts on target cells via binding to heterodimeric cell surface receptors (IFN-γ-R), with resulting intracellular signals delivered via activation of JAK1 and JAK2 tyrosine kinases that associate with IFN-γ-R1 and IFN-γ-R2 subunits, respectively, and subsequent activation and translocation of STAT-1 to the nucleus (100). STAT-1 is also a central mediator of IL-27 signaling (101), while STAT-3 and STAT-4 mediate intracellular signaling by other potent antitumor cytokines including IL-12 and IL-23 (102, 103). The present studies have now demonstrated decreased expression of the genes that encode several key signaling intermediates that are critical components of an evolving antitumor immune response. These include diminished expression of several key components of signaling pathways that mediate the effects of IFN-γ including the IFN-γ receptor, JAK1, JAK2, and STAT-1 within POB CM and POB UN series tumors. We also noted substantial decreases in the expression of genes encoding IL-18 as well as *Stat-3* and *Stat-4* within these tumors. Further, as has been described previously in human neuroblastoma cells (104, 105), we have found marked reductions in the expression of the gene encoding β_2-microglobulin, a key component of MHC class I T-cell receptor antigen recognition complex. These patterns of gene expression suggest that POB CM and POB UN series tumors could possess multiple alterations that could confer a resistance to host immune response mechanisms, in particular those mechanisms that are mediated by IFN-γ.

Cheng *et al*. described the ability to generate a series of isogenic cell lines from the original TH-MYCN transgenic mouse strain and analyzed their growth in Nude mice (nu/nu). Tumors were suspended in Matrigel and were injected subcutaneously. Although their analysis centered on cytogeneics and ploidy, they did describe increased MYCN (as expected in a transgenic model), *odc* (ornithine decarboxylase), *mrp1*, TH (tyrosine hydroxylase), and S100A6 gene expression. Our work confirms their finding of TH expression. We did find ODC mRNA overexpression

RIGHTSLINK

as found in our database (http://pob.abcc.ncifcrf.gov/cgi-bin/JK), which will be released upon publication. We also found that S100A6 expressed very highly in some normal tissue, giving the appearance of low expression in our transplantable or spontaneously arising tumors. However, our demonstration of increased catecholamine production provides confirmation of the neuroblastoma origin of these samples and is relevant to the clinical disease, and supports their findings at the functional level. Our work differed in that we focused on an orthotopic transplantation within the same strain, and focused on using gene expression array and detailed pathological analysis to validate the similarity of these tumors to those arising spontaneously.

Neuroblastoma is a complex disease with different gene sets associated with stage, prognosis, and MYCN+ versus MYCN(–) disease. Nevertheless, our previously published analysis of patient tumors with poor outcome identified both Robo2 and Slit3 as preferentially expressed transcripts in human disease, correlating with the finding of Robo1 and Slit2 in this report (25). Fischer *et al*. identified Robo1 as being associated with poor outcome as well (106). Two studies identified another of the genes we describe, survivin (BIRC5) as upregulated in advanced neuroblastoma (107, 108). In the report of Abel *et al*., a six-gene classification system for neuroblastoma was designed that includes another of the genes upregulated in our analysis, cyclinD1 (CCND1). If we include MYCN, our mouse tumors express 3 of the 6 genes they report as defining essential signatures for neuroblastoma subtypes. The use of the MYCN transgenic mouse has helped to define what the MYCN expression signature is, and our work contributes to this body of work (109, 110).

The present studies demonstrate a unique approach by utilizing spontaneous tumors in transgenic mice as a source for the derivation of novel transplantable neuroblastoma tumor cell lines, an approach that may be reasonably applied to the development of a broad range of transplantable orthotopic tumor models from transgenic mice. In this report, we demonstrate that established orthotopic POB CM and POB UN series tumors possess a wide range of biochemical, histopathologic, and molecular features that are consistent with both spontaneous MYCN transgenic neuroblastoma tumors, and conventional features of human neuroblastoma tumors as well. We have also demonstrated the integrated use of cDNA microarray for high-throughput characterization of patterns of gene expression within POB CM and POB UN series tumors and validation of the expression of potential therapeutic targets (Cdk4) at the protein level within the microenvironment of these tumors using tumor tissue arrays. The expression profile of these tumors highlights their potential utility as model systems for investigation of several aspects of the biology of neuroblastoma tumors *in vivo*, and for preclinical investigation of novel therapeutic agents that target the regulation of pathways including apoptosis, angiogenesis, cell cycle progression, and metastasis. Further, observed reductions in the expression of several genes that may mediate the responsiveness of tumor cells to the host immune response, including components of the IFN-γ signaling pathway, suggest that these tumors may afford particularly challenging models for the investigation of immunotherapeutic approaches for the treatment of neuroblastoma. Collectively, the current report describes important new tools for drug discovery, and more specifically, for the investigation of novel approaches for the treatment of advanced neuroblastoma.

ACKNOWLEDGMENTS

The authors would like to thank Ms. Susan Charbonneau and Lin Grove, for assistance with manuscript preparation, and Rimas Orentas for editing the manuscript. These studies were supported (in part) by the Intramural Program, National Institutes of Health, Center for Cancer Research, National Cancer Institute, Bethesda, MD, USA. The generous support of these studies by the Children's Cancer Foundation is also gratefully acknowledged. The content of this publication does not necessarily reflect the views or policies of the Department of Health and Human Services, nor does mention of trade names, commercial products, or organizations imply endorsement by the US Government. This project has been funded in whole or in part with Federal funds from the National Cancer Institute, National Institutes of Health, under contract no. N01-CO-12400. Animal care was provided in accordance with the procedures outlined in the *Guide for the Care and Use of Laboratory Animals* (National Institutes of Health, Publication No. 86-23, 1985).

DECLARATION OF INTEREST

The authors have no declarations of interest or conflict of interest.

REFERENCES

1. Brodeur GM, Maris JM. Neuroblastoma. In Principles and Practice of Pediatric Oncology, PA Pizzo and DG Poplack (eds.). Philadelphia, PA: Lippincott William & Wilkins, 2002:895–938.
2. Brodeur GM. Neuroblastoma: biological insights into a clinical enigma. Nat Rev Cancer 2003;3:203–216.
3. Goldsby RE, Matthay KK. Neuroblastoma: evolving therapies for a disease with many faces. Paediatr Drugs 2004;6:107–122.
4. Weinstein JL, Katzenstein HM, Cohn SL. Advances in the diagnosis and treatment of neuroblastoma. Oncologist 2003;8:278–292.
5. Wigginton J. Preclinical animal models for the investigation of biologic approaches for the therapy of neuroblastoma. In Renal and Adrenal Tumors: Biology and Management, A Belldegrun, R Figlin, D Vaughn, A Ritchie, and T Oliver (eds.). New York: Oxford University Press, 2003, 144–155.
6. Lode HN, Dreier T, Xiang R, Varki NM, Kang AS, Reisfeld RA. Gene therapy with a single chain interleukin 12 fusion protein induces T cell-dependent protective immunity in a syngeneic model of murine neuroblastoma. Proc Natl Acad Sci U S A 1998;95:2475–2480.
7. Lode HN, Xiang R, Varki NM, Dolman CS, Gillies SD, Reisfeld RA. Targeted interleukin-2 therapy for spontaneous neuroblastoma metastases to bone marrow. J Natl Cancer Inst 1997;89:1586–1594.
8. Katsanis E, Blazar BR, Bausero MA, Gunther R, Anderson PM. Retroperitoneal inoculation of murine neuroblastoma results in a reliable model for evaluation of the antitumor immune response. J Pediatr Surg 1994;29:538–542.
9. Katsanis E, Bausero MA, Panoskaltsis-Mortari A, Dancisak BB, Xu Z, Orchard PJ, Davis CG, Blazar BR. Irradiation of singly and

Cancer Invest Downloaded from informahealthcare.com by NIH Pathology Lab on 11/12/14
For personal use only.

RIGHTSLINK

doubly transduced murine neuroblastoma cells expressing B7-1 and producing interferon-gamma reduces their capacity to induce systemic immunity. Cancer Gene Ther 1996;3:75–82.
10. Fowler C, Zimmer C, Boghaert E, Thomas M, Zimmer S. Metastasis of C1300 and TBJ murine neuroblastomas correlates with expression of matrix metalloproteinases. Cancer Lett 1995;93:171–177.
11. Shimizu T, Berhanu A, Redlinger RE, , Watkins S, Lotze MT, Barksdale EM, Interleukin-12 transduced dendritic cells induce regression of established murine neuroblastoma. J Pediatr Surg 2001;36:1285–1292.
12. Brodeur GM, Seeger RC, Schwab M, Varmus HE, Bishop JM. Amplification of N-myc in untreated human neuroblastomas correlates with advanced disease stage. Science 1984;224:1121–1124.
13. Seeger RC, Brodeur GM, Sather H, Dalton A, Siegel SE, Wong KY, Hammond D. Association of multiple copies of the N-myc oncogene with rapid progression of neuroblastomas. N Engl J Med 1985;313:1111–1116.
14. Weiss WA, Aldape K, Mohapatra G, Feuerstein BG, Bishop JM. Targeted expression of MYCN causes neuroblastoma in transgenic mice. EMBO J 1997;16:2985–2995.
15. Okabe M, Ikawa M, Kominami K, Nakanishi T, Nishimune Y. "Green mice" as a source of ubiquitous green cells. FEBS Lett 1997;407:313–319.
16. Khan T, Hixon JA, Stauffer JK, Lincoln E, Back TC, Brenner J, Lockett S, Nagashima K, Powell D, Wigginton JM. Therapeutic modulation of Akt activity and antitumor efficacy of interleukin-12 against orthotopic murine neuroblastoma. J Natl Cancer Inst 2006;98:190–202.
17. Salcedo R, Stauffer JK, Lincoln E, Back TC, Hixon JA, Hahn C, Shafer-Weaver K, Malyguine A, Kastelein R, Wigginton JM. IL-27 mediates complete regression of orthotopic primary and metastatic murine neuroblastoma tumors: role for CD8+ T cells. J Immunol 2004;173:7170–7182.
18. Motoike T, Loughna S, Perens E, Roman BL, Liao W, Chau TC, Richardson CD, Kawate T, Kuno J, Weinstein BM, Stainier DY, Sato TN. Universal GFP reporter for the study of vascular development. Genesis 2000;28:75–81.
19. Eisenhofer G, Goldstein DS, Stull R, Keiser HR, Sunderland T, Murphy DL, Kopin IJ. Simultaneous liquid-chromatographic determination of 3,4-dihydroxyphenylglycol, catecholamines, and 3,4-dihydroxyphenylalanine in plasma, and their responses to inhibition of monoamine oxidase. Clin Chem 1986;32:2030–2033.
20. Stauffer JK, Khan T, Salcedo R, Hixon JA, Lincoln E, Back TC, Wigginton JM. Multicolor fluorescence-based approaches for imaging cytokine-induced alterations in the neovascularization, growth, metastasis, and apoptosis of murine neuroblastoma tumors. J Immunother 2006;29:151–164.
21. Wigginton JM, Gruys E, Geiselhart L, Subleski J, Komschlies KL, Park JW, Wiltrout TA, Nagashima K, Back TC, Wiltrout RH. IFN-gamma and Fas/FasL are required for the antitumor and antiangiogenic effects of IL-12/pulse IL-2 therapy. J Clin Invest 2001;108:51–62.
22. Wei J, Khan J. Purification of total RNA from mammalian cells and tissues. In DNA Microarays: A Molecular Cloning Manual, D Botwell and J Sambrook (eds.). Cold Spring Harbor, NY: Cold Spring Harbor Press, 2002, 110–119.
23. Sotiriou C, Khanna C, Jazaeri AA, Petersen D, Liu ET. Core biopsies can be used to distinguish differences in expression profiling by cDNA microarrays. J Mol Diagn 2002;4:30–36.
24. Hegde P, Qi R, Abernathy K, Gay C, Dharap S, Gaspard R, Hughes JE, Snesrud E, Lee N, Quackenbush J. A concise guide to cDNA microarray analysis. Biotechniques 2000;29:548–550; 52–54, 56 passim.
25. Wei JS, Greer BT, Westermann F, Steinberg SM, Son CG, Chen QR, Whiteford CC, Bilke S, Krasnoselsky AL, Cenacchi, N, Catchpoole D, Berthold F, Schwab M, Khan J. Prediction of clinical outcome using gene expression profiling and artificial neural networks for patients with neuroblastoma. Cancer Res 2004;64:6883–6891.
26. Krasnoselsky AL, Whiteford CC, Wei JS, Bilke S, Westermann F, Chen QR, Khan J. Altered expression of cell cycle genes distinguishes aggressive neuroblastoma. Oncogene 2005;24:1533–1541.
27. Tusher VG, Tibshirani R, Chu G. Significance analysis of microarrays applied to the ionizing radiation response. Proc Natl Acad Sci U S A 2001;98:5116–5121.
28. Meitar D, Crawford SE, Rademaker AW, Cohn SL. Tumor angiogenesis correlates with metastatic disease, N-myc amplification, and poor outcome in human neuroblastoma. J Clin Oncol 1996;14:405–414.
29. Stickler GB, Flock EV. Neuroblastoma and ganglioneuroblastoma: associated increased urinary excretion of catecholamines. Cancer Chemother Rep 1962;16:439–442.
30. Voorhess ML, Gardner LI. The value of serial catecholamine determinations in children with neuroblastoma. Pediatrics 1962;30:241–246.
31. Matthay KK, Villablanca JG, Seeger RC, Stram DO, Harris RE, Ramsay NK, Swift P, Shimada H, Black CT, Brodeur GM, Gerbing RB, Reynolds CP. Treatment of high-risk neuroblastoma with intensive chemotherapy, radiotherapy, autologous bone marrow transplantation, and 13-cis-retinoic acid. Children's Cancer Group. N Engl J Med 1999;341:1165–1173.
32. Gilman AL, Ozkaynak MF, Matthay KK, Krailo M, Yu AL, Gan J, Sternberg A, Hank JA, Reaman GH, Sondel PM. Phase I study of ch14.18 with granulocyte-macrophage colony-stimulating factor and interleukin-2 in children with neuroblastoma after autologous bone marrow transplantation or stem-cell rescue: a report from the Children's Oncology Group. J Clin Oncol 2009;27:85–91.
33. Shimada H, Umehara S, Monobe Y, Hachitanda Y, Nakagawa A, Goto S, Gerbing RB, Stram DO, Lukens JM, Mathtay KK. International neuroblastoma pathology classification for prognostic evaluation of patients with peripheral neuroblastic tumors: a report from the Children's Cancer Group. Cancer 2001;92:2451–2461.
34. Shimada H, Ambros IM, Dehner LP, Hata J, Joshi VV, Roald B. Terminology and morphologic criteria of neuroblastic tumors: recommendations by the International Neuroblastoma Pathology Committee. Cancer 1999;86:349–363.
35. LaBrosse EH, Comoy E, Bohuon C, Zucker JM, Schweisguth O. Catecholamine metabolism in neuroblastoma. J Natl Cancer Inst 1976;57:633–638.
36. Pritchard J, Barnes J, Germond S, Hartman O, de Kraker J, Lewis I, Lockwood L, Wallendszus K. Stage and urinary catecholamine metabolite excretion in neuroblastoma. European Neuroblastoma Study Group. Lancet 1989;2:514–515.
37. Ribatti D, Ponzoni M. Antiangiogenic strategies in neuroblastoma. Cancer Treat Rev 2005;31:27–34.
38. Shusterman S, Maris JM. Prospects for therapeutic inhibition of neuroblastoma angiogenesis. Cancer Lett 2005;228:171–179.
39. Streck CJ, Ng CY, Zhang Y, Zhou J, Nathwani AC, Davidoff AM. Interferon-mediated anti-angiogenic therapy for neuroblastoma. Cancer Lett 2005;228:163–170.
40. Wang B, Xiao Y, Ding BB, Zhang N, Yuan X, Gui L, Qian KX, Duan S, Chen Z, Rao Y, Geng JG. Induction of tumor angiogenesis by Slit-Robo signaling and inhibition of cancer growth by blocking Robo activity. Cancer Cell 2003;4:19–29.
41. Wong K, Park HT, Wu JY, Rao Y. Slit proteins: molecular guidance cues for cells ranging from neurons to leukocytes. Curr Opin Genet Dev 2002;12:583–591.
42. Wang KH, Brose K, Arnott D, Kidd T, Goodman CS, Henzel W, Tessier-Lavigne M. Biochemical purification of a mammalian slit protein as a positive regulator of sensory axon elongation and branching. Cell 1999;96:771–784.

Cancer Invest Downloaded from informahealthcare.com by NIH Pathology Lab on 11/12/14
For personal use only.

RIGHTSLINK

43. Wu W, Wong K, Chen J, Jiang Z, Dupuis S, Wu JY, Rao Y. Directional guidance of neuronal migration in the olfactory system by the protein Slit. Nature 1999;400:331–336.
44. Gao AG, Lindberg FP, Finn MB, Blystone SD, Brown EJ, Frazier WA. Integrin-associated protein is a receptor for the C-terminal domain of thrombospondin. J Biol Chem 1996;271:21–24.
45. Good DJ, Polverini PJ, Rastinejad F, Le Beau MM, Lemons RS, Frazier WA, et al. A tumor suppressor-dependent inhibitor of angiogenesis is immunologically and functionally indistinguishable from a fragment of thrombospondin. Proc Natl Acad Sci U S A 1990;87:6624–6628.
46. Yang QW, Liu S, Tian Y, Salwen HR, Chlenski A, Weinstein J, et al. Methylation-associated silencing of the thrombospondin-1 gene in human neuroblastoma. Cancer Res 2003;63:6299–6310.
47. Castle VP, Ou X, O'Shea S, Dixit VM. Induction of thrombospondin 1 by retinoic acid is important during differentiation of neuroblastoma cells. J Clin Invest 1992;90:1857–1863.
48. Miyashita M, Ohnishi H, Okazawa H, Tomonaga H, Hayashi A, Fujimoto TT, Furuya N, Matozaki T. Promotion of neurite and filopodium formation by CD47: roles of integrins, Rac, and Cdc42. Mol Biol Cell 2004;15:3950–3963.
49. Handsley MM, Edwards DR. Metalloproteinases and their inhibitors in tumor angiogenesis. Int J Cancer 2005;115:849–860.
50. Stetler-Stevenson WG, Seo DW. TIMP-2: an endogenous inhibitor of angiogenesis. Trends Mol Med 2005;11:97–103.
51. Ara T, Fukuzawa M, Kusafuka T, Komoto Y, Oue T, Inoue M, Okada A. Immunohistochemical expression of MMP-2, MMP-9, and TIMP-2 in neuroblastoma: association with tumor progression and clinical outcome. J Pediatr Surg 1998;33:1272–1278.
52. Spurbeck WW, Ng CY, Strom TS, Vanin EF, Davidoff AM. Enforced expression of tissue inhibitor of matrix metalloproteinase-3 affects functional capillary morphogenesis and inhibits tumor growth in a murine tumor model. Blood 2002;100: 3361–3368.
53. Spurbeck WW, Ng CY, Vanin EF, Davidoff AM. Retroviral vector-producer cell-mediated in vivo gene transfer of TIMP-3 restricts angiogenesis and neuroblastoma growth in mice. Cancer Gene Ther 2003;10:161–167.
54. Iolascon A, Borriello A, Giordani L, Cucciolla V, Moretti A, Monno F, Criniti V, Marzullo A, Criscuolo M, Garione FD. Caspase 3 and 8 deficiency in human neuroblastoma. Cancer Genet Cytogenet 2003;146:41–47.
55. Teitz T, Wei T, Valentine MB, Vanin EF, Grenet J, Valentine VA, Behm FG, Lahti JM, Kidd VJ. Caspase 8 is deleted or silenced preferentially in childhood neuroblastomas with amplification of MYCN. Nat Med 2000;6:529–535.
56. Koizumi H, Ohkawa I, Tsukahara T, Momoi T, Nakada K, Uchikoshi T. Apoptosis in favourable neuroblastomas is not dependent on Fas (CD95/APO-1) expression but on activated caspase 3 (CPP32). J Pathol 1999;189:410–415.
57. Adida C, Berrebi D, Peuchmaur M, Reyes-Mugica M, Altieri DC. Anti-apoptosis gene, survivin, and prognosis of neuroblastoma. Lancet 1998;351:882–883.
58. Islam A, Kageyama H, Takada N, Kawamoto T, Takayasu H, Isogai E, Ohira M, Hashizume K, Kobayashi H, Kaneko Y, Nakagawara A. High expression of Survivin, mapped to 17q25, is significantly associated with poor prognostic factors and promotes cell survival in human neuroblastoma. Oncogene 2000;19:617–623.
59. van Golen CM, Castle VP, Feldman EL. IGF-I receptor activation and BCL-2 overexpression prevent early apoptotic events in human neuroblastoma. Cell Death Differ 2000;7:654–665.
60. Poulaki V, Mitsiades N, Romero ME, Tsokos M. Fas-mediated apoptosis in neuroblastoma requires mitochondrial activation and is inhibited by FLICE inhibitor protein and Bcl-2. Cancer Res 2001;61:4864–4872.
61. Ho R, Eggert A, Hishiki T, Minturn JE, Ikegaki N, Foster P, Camoratto AM, Evans AE, Brodeur GM. Resistance to chemotherapy mediated by TrkB in neuroblastomas. Cancer Res 2002;62:6462–6466.
62. Kim S, Kang J, Hu W, Evers BM, Chung DH. Geldanamycin decreases Raf-1 and Akt levels and induces apoptosis in neuroblastomas. Int J Cancer 2003;103:352–359.
63. Kim S, Kang J, Qiao J, Thomas RP, Evers BM, Chung DH. Phosphatidylinositol 3-kinase inhibition down-regulates survivin and facilitates TRAIL-mediated apoptosis in neuroblastomas. J Pediatr Surg 2004;39:516–521.
64. Shankar SL, Mani S, O'Guin KN, Kandimalla ER, Agrawal S, Shafit-Zagardo B. Survivin inhibition induces human neural tumor cell death through caspase-independent and -dependent pathways. J Neurochem 2001;79:426–436.
65. Bown N, Lastowska M, Cotterill S, O'Neill S, Ellershaw C, Roberts P, Lewis I, Pearson AD. 17q gain in neuroblastoma predicts adverse clinical outcome. U.K. Cancer Cytogenetics Group and the U.K. Children's Cancer Study Group. Med Pediatr Oncol 2001;36:14–19.
66. Lastowska M, Cotterill S, Bown N, Cullinane C, Variend S, Lunec J, Strachan T, Pearson AD, Lackson MS. Breakpoint position on 17q identifies the most aggressive neuroblastoma tumors. Genes Chromosomes Cancer 2002;34:428–436.
67. Pratt MA, Niu M, White D. Differential regulation of protein expression, growth and apoptosis by natural and synthetic retinoids. J Cell Biochem 2003;90:692–708.
68. Goldsmith KC, Hogarty MD. Targeting programmed cell death pathways with experimental therapeutics: opportunities in high-risk neuroblastoma. Cancer Lett 2005;228:133–141.
69. Zaffaroni N, Pennati M, Daidone MG. Survivin as a target for new anticancer interventions. J Cell Mol Med 2005;9:360–372.
70. Emanuel S, Rugg CA, Gruninger RH, Lin R, Fuentes-Pesquera A, Connolly PJ, Wetter SK, Hollister B, Kruger WW, Napier C, Jolliffe, Middleton SA. The in vitro and in vivo effects of JNJ-7706621: a dual inhibitor of cyclin-dependent kinases and aurora kinases. Cancer Res 2005;65:9038–9046.
71. Young MA, Shah NP, Chao LH, Seeliger M, Milanov ZV, Biggs WH, 3rd, Treiber DK, Patel HK, Zarrinkar PP, Lockart DJ, Sawyers CL, Kuriyan J. Structure of the kinase domain of an imatinib-resistant Abl mutant in complex with the Aurora kinase inhibitor VX-680. Cancer Res 2006;66:1007–1014.
72. Banerji U, O'Donnell A, Scurr M, Pacey S, Stapleton S, Asad Y, Simmons L, Mloney A, Raynaud F, Campbell M, Walton M, Lakhani, Kaye S, Workman P, Judson I. Phase I pharmacokinetic and pharmacodynamic study of 17-allylamino, 17-demethoxygeldanamycin in patients with advanced malignancies. J Clin Oncol 2005;23:4152–4161.
73. Xiao HH, Makeyev Y, Butler J, Vikram B, Franklin WA. 7-Hydroxystaurosporine (UCN-01) preferentially sensitizes cells with a disrupted TP53 to gamma radiation in lung cancer cell lines. Radiat Res 2002;158:84–93.
74. Eckerdt F, Yuan J, Strebhardt K. Polo-like kinases and oncogenesis. Oncogene 2005;24:267–276.
75. Gumireddy K, Reddy MV, Cosenza SC, Boominathan R, Baker SJ, Papathi N, Jiang J, Holland J, Reddy EP. ON01910, a non-ATP-competitive small molecule inhibitor of Plk1, is a potent anticancer agent. Cancer Cell 2005;7:275–286.
76. Shapiro GI. Preclinical and clinical development of the cyclin-dependent kinase inhibitor flavopiridol. Clin Cancer Res 2004;10:4270s–4275s.
77. Swanton C. Cell-cycle targeted therapies. Lancet Oncol 2004; 5:27–36.
78. Dong JT, Lamb PW, Rinker-Schaeffer CW, Vukanovic J, Ichikawa T, Isaacs JT, Barrett JC. KAI1, a metastasis suppressor gene for prostate cancer on human chromosome 11p11.2. Science 1995;268:884–886.
79. Cowin P, Rowlands TM, Hatsell SJ. Cadherins and catenins in breast cancer. Curr Opin Cell Biol 2005;17:499–508.
80. Nelson WJ, Nusse R. Convergence of Wnt, beta-catenin, and cadherin pathways. Science 2004;303:1483–1487.

Cancer Invest Downloaded from informahealthcare.com by NIH Pathology Lab on 11/12/14
For personal use only.

RIGHTSLINK

81. Wheelock MJ, Johnson KR. Cadherins as modulators of cellular phenotype. Annu Rev Cell Dev Biol 2003;19:207–235.
82. Reed CC, Waterhouse A, Kirby S, Kay P, Owens RT, McQuillan DJ, Iozzo RV. Decorin prevents metastatic spreading of breast cancer. Oncogene 2005;24:1104–1110.
83. Ikeyama S, Koyama M, Yamaoko M, Sasada R, Miyake M. Suppression of cell motility and metastasis by transfection with human motility-related protein (MRP-1/CD9) DNA. J Exp Med 1993;177:1231–1237.
84. Cox JL, Sexton PS, Green TJ, Darmani NA. Inhibition of B16 melanoma metastasis by overexpression of the cysteine proteinase inhibitor cystatin C. Melanoma Res 1999;9:369–374.
85. Aryee DN, Ambros I, Ambros PF, Muehlbacher K, Luegmayr A, Yoshie O, Kovar Het al. Frequent low level expression in Ewing sarcoma family tumors and widespread absence of the metastasis suppressor KAI1/CD82 in neuroblastoma. Pediatr Res 2002;52: 279–285.
86. Fazili Z, Sun W, Mittelstaedt S, Cohen C, Xu XX. Disabled-2 inactivation is an early step in ovarian tumorigenicity. Oncogene 1999;18:3104–3113.
87. Hsieh SY, Hsieh PS, Chiu CT, Chen WY. Dickkopf-3/REIC functions as a suppressor gene of tumor growth. Oncogene 2004;23:9183–9189.
88. Dang DT, Chen X, Feng J, Torbenson M, Dang LH, Yang VW. Overexpression of Kruppel-like factor 4 in the human colon cancer cell line RKO leads to reduced tumorigenecity. Oncogene 2003;22:3424–3430.
89. Li Y, Pei J, Xia H, Ke H, Wang H, Tao W. Lats2, a putative tumor suppressor, inhibits G1/S transition. Oncogene 2003;22:4398–4405.
90. Deng Y, Yao L, Chau L, Ng SS, Peng Y, Liu X, Au WS, Wang J, Li F, Ji S, Han H, Lie X, Li Q, Kung HF, Leung SY, Lin MC. N-Myc downstream-regulated gene 2 (NDRG2) inhibits glioblastoma cell proliferation. Int J Cancer 2003;106:342–347.
91. Rossi M, Sayan AE, Terrinoni A, Melino G, Knight RA. Mechanism of induction of apoptosis by p73 and its relevance to neuroblastoma biology. Ann N Y Acad Sci 2004;1028: 143–149.
92. Terrinoni A, Ranalli M, Cadot B, Leta A, Bagetta G, Vousden KH, Melino G. p73-alpha is capable of inducing scotin and ER stress. Oncogene 2004;23:3721–3725.
93. Karim R, Tse G, Putti T, Scolyer R, Lee S. The significance of the Wnt pathway in the pathology of human cancers. Pathology 2004;36:120–128.
94. Moon RT, Kohn AD, De Ferrari GV, Kaykas A. WNT and beta-catenin signalling: diseases and therapies. Nat Rev Genet 2004;5:691–701.
95. Blanc E, Roux GL, Benard J, Raguenez G. Low expression of Wnt-5a gene is associated with high-risk neuroblastoma. Oncogene 2005;24:1277–1283.
96. Kaplan DH, Shankaran V, Dighe AS, Stockert E, Aguet M, Old LJ, Schreiber RD. Demonstration of an interferon gamma-dependent tumor surveillance system in immunocompetent mice. Proc Natl Acad Sci U S A 1998;95:7556–7561.
97. Nastala CL, Edington HD, McKinney TG, Tahara H, Nalesnik MA, Brunda MJ, Gately MK, Wolf SF, Schreiber RD, Storkus WJ. Recombinant IL-12 administration induces tumor regression in association with IFN-gamma production. J Immunol 1994;153:1697–1706.
98. Wigginton JM, Lee JK, Wiltrout TA, Alvord WG, Hixon JA, Subleski J, Back TC, Wiltrout RH. Synergistic engagement of an ineffective endogenous anti-tumor immune response and induction of IFN-gamma and Fas-ligand-dependent tumor eradication by combined administration of IL-18 and IL-2. J Immunol 2002;169:4467–4474.
99. Hisada M, Kamiya S, Fujita K, Belladonna ML, Aoki T, Koyanagi Y, Mizugucho J, Yoshito T. Potent antitumor activity of interleukin-27. Cancer Res 2004;64:1152–1156.
100. Schroder K, Hertzog PJ, Ravasi T, Hume DA. Interferon-gamma: an overview of signals, mechanisms and functions. J Leukoc Biol 2004;75:163–189.
101. Takeda A, Hamano S, Yamanaka A, Hanada T, Ishibashi T, Mak TW, Yoshimura A, Yoshida H. Cutting edge: role of IL-27/WSX-1 signaling for induction of T-bet through activation of STAT1 during initial Th1 commitment. J Immunol 2003;170:4886–4890.
102. Parham C, Chirica M, Timans J, Vaisberg E, Travis M, Cheung J, Pflanz S, Zhang R, Singh KP, Vega F, To W, Wagner J, O'Farrell AM, McClanahan T, Zurawski S, Hannum C, Gorman D, Rennick DM, Kastelein RA, de Wall Malefyt R, Moore KW. A receptor for the heterodimeric cytokine IL-23 is composed of IL-12Rbeta1 and a novel cytokine receptor subunit, IL-23R. J Immunol 2002;168:5699–5708.
103. Watford WT, Hissong BD, Bream JH, Kanno Y, Muul L, O'Shea JJ. Signaling by IL-12 and IL-23 and the immunoregulatory roles of STAT4. Immunol Rev 2004;202:139–156.
104. Lampson LA, Fisher CA. Weak HLA and beta 2-microglobulin expression of neuronal cell lines can be modulated by interferon. Proc Natl Acad Sci U S A 1984;81:6476–6480.
105. Whelan JP, Chatten J, Lampson LA. HLA class I and beta 2-microglobulin expression in frozen and formaldehyde-fixed paraffin sections of neuroblastoma tumors. Cancer Res 1985;45:5976–5983.
106. Fischer M, Oberthuer A, Brors B, Kahlert Y, Skowron M, Voth H, Warnat P, Emestus K, Berthold F. Differential expression of neuronal genes defines subtypes of disseminated neuroblastoma with favorable and unfavorable outcome. Clin Cancer Res 2006;12:5118–5128.
107. Vermeulen J, De Preter K, Naranjo A, Vercruysse L, Van Roy N, Hellemans J, Swerts K, Bravo S, Scaruffi P, Tonini GP, De Bernardi B, Noguera R, Piqueras M, Canete A, Castel V, Janoueix-Lerosey I, Delattre O, Schleiermacher G, Michon J, Combaret V, Fischer M, Oberthuer A, Ambros PF, Beiske K, Denard J, Marques B, Rubie H, Kohler J, Potschger U, Ladenstain R, Hogarty MD, McGrady P, London WB, Laureys G, Speleman F, Vandesompele J. Predicting outcomes for children with neuroblastoma using a multigene-expression signature: a retrospective SIOPEN/COG/GPOH study. Lancet Oncol 2009;10:663–671.
108. Abel F, Dalevi D, Nethander M, Jornsten R, De Preter K, Vermeulen J, Stallings R, Kogner P, Maris J, Nilsson S. A 6-gene signature identifies four molecular subgroups of neuroblastoma. Cancer Cell Int 2011;11:9.
109. Hackett CS, Hodgson JG, Law ME, Fridlyand J, Osoegawa K, de Jong PJ, Nowak NJ, Pinkel D, Albertson DG, Jain A, Jenkins R, Gray JW, Weiss WA. Genome-wide array CGH analysis of murine neuroblastoma reveals distinct genomic aberrations which parallel those in human tumors. Cancer Res 2003;63:5266–5273.
110. Cheng AJ, Cheng NC, Ford J, Smith J, Murray JE, Flemming C, Lastowska M, Jackson MS, Mackett CS, Weiss WA, Marshall GM, Kees UR, Norris MD, Haber M. Cell lines from MYCN transgenic murine tumours reflect the molecular and biological characteristics of human neuroblastoma. Eur J Cancer 2007;43:1467–1475.

Cancer Invest Downloaded from informahealthcare.com by NIH Pathology Lab on 11/12/14
For personal use only.

RIGHTSLINK